Original scientific paper
https://doi.org/10.33180/InfMIDEM2022.404

Informacije MIDEM
Journal of Microelectronics,
Electronic Components and Materials
Vol. 52, No. 4(2022), 239 – 262

Mixed-mode Universal Filter Using FD-CCCTA and its Extension as Shadow Filter

Divya Singh, Sajal K. Paul*

Department of Electronics Engineering, Indian Institute of Technology (Indian School of Mines), Dhanbad, Jharkhand, India

Abstract: This paper presents a fully differential current conveyor cascaded transconductance amplifier (FD-CCCTA), a modified FD-second generation current conveyor (FD-CCII) version. After that, a novel mixed-mode universal filter (UF) is developed employing only one FD-CCCTA. It results in all the four modes of UFs, namely current mode (CM), voltage mode (VM), transimpedance mode (TIM), and transadmittance mode (TAM). Moreover, this filter topology is extended to two mixed-mode universal shadow filters. The first shadow filter topology realizes the VM and CM universal filters. The second mixed-mode universal shadow filter realizes all four modes. The proposed shadow filters add flexibility in the orthogonal tuning of filter parameters, ω_0 and Q_0. Further, the gain of the shadow filter can be tuned electronically. Matching constraint is not required in any of the filters. The functional verifications have been performed using TSMC 180 nm technology in cadence virtuoso spectre.

Keywords: FD-CCCTA; FD-CCII; mixed-mode; shadow-filter

Univerzalni filter z mešanim načinom uporabe FD-CCCTA in njegova razširitev kot filter v senci

Izvleček: Članek predstavlja popolnoma diferencialni kaskadni transkondukcijski ojačevalnik (FD-CCCTA), modificirano različico tokovnega transporterja FD druge generacije (FD-CCII). Razvit nov univerzalni filter (UF) z mešanim načinom delovanja, ki uporablja samo en FD-CCCTA. Rezultat so vsi štirje načini UF, in sicer tokovni način (CM), napetostni način (VM), transimpedančni način (TIM) in transadmitančni način (TAM). Poleg tega je ta topologija filtra razširjena na dva univerzalna senčna filtra z mešanim načinom delovanja. Prva topologija senčnega filtra izvaja univerzalna filtra VM in CM. Drugi univerzalni filter v senci z mešanim načinom delovanja omogoča vse štiri načine delovanja. Predlagani filtri v senci povečujejo fleksibilnost pri ortogonalnem nastavljanju parametrov filtra, ω_0 in Q_0. Poleg tega je mogoče elektronsko nastaviti ojačenje filtra v senci. Pri nobenem od filtrov ni potrebna omejitev ujemanja. Funkcionalna preverjanja so bila izvedena s 180 nm tehnologijo TSMC v programu cadence virtuoso spectre.

Ključne besede: FD-CCCTA; FD-CCII; mešani način; filter senc

** Corresponding Author's e-mail: divs0508singh@gmail.com*

1 Introduction

Mixed-mode filters with all the responses of current-mode (CM) (both the input and output as a current), voltage- mode (VM) (both the input and output as a voltage), transimpedance-mode (TIM) (input as a current and output as a voltage), and transadmittance-mode (TAM) (input as a voltage and output as a current) are very much desirable in the analog signal processing, communication, and instrumentation [1]. At the same time, TAM and TIM filters play a vital role in the circuits which intends to connect the current mode circuits to the voltage mode circuits and vice-versa. TAM and TIM avoid the unnecessary circuitry requirement during V-I interfacing and the improvement in the effectiveness of the circuit. It concludes that the mixed-mode filters with all the four modes present in the same topology provide ample flexibility for analog circuit design. Few single-input-multiple-output (SIMO) mixed-mode universal filter topologies are available in the literature. SIMO [2] has got

How to cite:
D. Singh et al., "Mixed-mode Universal Filter Using FD-CCCTA and its Extension as Shadow Filter", Inf. Midem-J. Microelectron. Electron. Compon. Mater., Vol. 52, No. 4(2022), pp. 239–262

an advantage over single-input-single-output (SISO), multiple-input-multiple-output (MIMO), and multiple input single output (MISO) because of the availability of all the responses simultaneously. The topology [3] uses two fully differential second-generation current conveyors (FDCCIIs) with floating passive elements as four resistors and two capacitors to realize the UF in VM and TIM while multifunction filters in TAM and CM. It also requires matching components. Another three CC-CCTAs based mixed-mode topology [4] provide LP, BP, and HP responses in CM and TIM, whereas LP, BP, HP, and BR responses in VM, and UF in TAM. In [5], four OTAs are used to realize LP, BP, and HP responses in TAM, TIM, CM, and LP responses in VM. The topology [6] uses six OTAs, one resistor, and two capacitors to realize UF in VM and TIM, whereas realizing BP and HP responses in TAM and BP, HP, and BR responses in CM. It possesses floating passive components and lacks independent tuning of filter parameters. Three differential difference current conveyors (DDCCs), four resistors, and two capacitors with matching components and floating passive elements realize UF in VM and TIM while LP, BP, and HP in TAM and CM in [7]. In [8], three dual voltage current conveyors (DVCCs), six MOSs, and two capacitors are used to realize LP, BP, and HP in CM and TAM, whereas LP, BP in TIM while LP, BP, and BR in VM with matching components requirement and no electronic tunability. Mixed-mode universal filter reported in [9] uses six operational transconductance amplifiers (OTAs). The topology [10] requires three four-terminal floating nullors (FTFNs), three resistors, and two capacitors to realize the low pass (LP), band pass (BP), and high pass (HP) simultaneously in all the modes without independent and electronic tuning. In [11], one FDCCII, three resistors, and two capacitors realize UF in VM and TIM, whereas BP and HP responses in TAM, and BP, HP, and, band reject (BR) responses in CM. It possesses floating passive elements and does not have an electronic tunability feature. Simultaneously three responses (LP, BP, and HP) in all the modes are proposed in [12] with the use of five multiple-output current-controlled conveyors (MCCCIIs) and two capacitors.

Reports of several shadow filters using various building blocks are available in the literature. However, among them, the majority are either in VM [13-20] or CM [21-28] and only one topology [29] is of TAM and TIM. To the best of the authors' knowledge, there is no SIMO mixed-mode universal shadow filter report.

The paper aims to present a novel mixed-mode universal filter employing only one FD-CCCTA. Further, this filter topology is extended to a universal shadow filter for all four modes to enhance the tunability and independent variation of ω and Q and provide tunable gains. The proposed circuit exhibits the following advantages: least number of active building blocks, no floating components, the simultaneous realization of various responses, no need for component matching constraints, and electronic and independent tuning of filter parameters, including gains. Moreover, the proposed circuit is the first SIMO mixed-mode universal shadow filter to the best of the authors' knowledge.

This paper consists of six sections. The introduction is given in Section 1, followed by section 2, which details the active building block FD-CCCTA. Section 3 describes the proposed circuit configuration, and Section 4 describes the non-ideality analysis. Section 5 compares the available literature, followed by Section 6, which discusses the functional verification.

2 Fully differential current conveyor cascaded transconductance amplifier (FD-CCCTA)

FD-CCCTA is a modified version of a fully differential second-generation current conveyor (FD-CCII) [30]. The symbol of FD-CCCTA is shown in Fig. 1, and its CMOS-based internal structure is shown in Fig. 2. It consists of six input terminals in the form of X as a low impedance terminal and Y as a high impedance terminal, while four output terminals in the form of Z and O as high impedance terminals. FD-CCCTA is designed using FD-CCII and transconductance amplifier (TA), where TA is used in the cascaded form, and therefore O terminal can be increased as per the requirement.

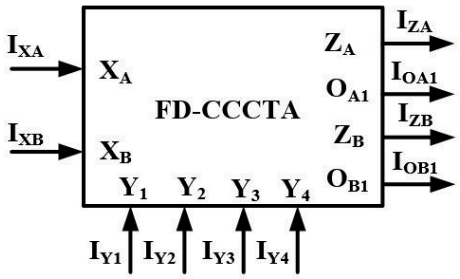

Figure 1: Symbol of FD-CCCTA.

The port relationships of FD-CCCTA can be expressed in matrix form as follows:

$$\begin{bmatrix} I_{Y1} \\ I_{Y2} \\ I_{Y3} \\ I_{Y4} \\ V_{XA} \\ V_{XB} \\ I_{ZA} \\ I_{ZB} \\ I_{OA1} \\ I_{OB1} \end{bmatrix} = \begin{bmatrix} 0 & 0 & 0 & 0 & 0 & 0 & 0 & 0 & 0 & 0 \\ 0 & 0 & 0 & 0 & 0 & 0 & 0 & 0 & 0 & 0 \\ 0 & 0 & 0 & 0 & 0 & 0 & 0 & 0 & 0 & 0 \\ 0 & 0 & 0 & 0 & 0 & 0 & 0 & 0 & 0 & 0 \\ 1 & -1 & 1 & 0 & 0 & 0 & 0 & 0 & 0 & 0 \\ -1 & 1 & 0 & 1 & 0 & 0 & 0 & 0 & 0 & 0 \\ 0 & 0 & 0 & 0 & 1 & 0 & 0 & 0 & 0 & 0 \\ 0 & 0 & 0 & 0 & 0 & 1 & 0 & 0 & 0 & 0 \\ 0 & 0 & 0 & 0 & 0 & 0 & g_{mA1} & 0 & 0 & 0 \\ 0 & 0 & 0 & 0 & 0 & 0 & 0 & g_{mB1} & 0 & 0 \end{bmatrix} \begin{bmatrix} V_{Y1} \\ V_{Y2} \\ V_{Y3} \\ V_{Y4} \\ I_{XA} \\ I_{XB} \\ V_{ZA} \\ V_{ZB} \\ V_{OA1} \\ V_{OB1} \end{bmatrix} \quad (1)$$

Where g_{mA1} and g_{mB1} are the transconductances of the transconductance amplifiers (TAs) connected at the Z_A and Z_B, respectively, can be expressed as:

$$g_{mA1} = \sqrt{\mu_n C_{ox} \left(\frac{W}{L}\right)_{M_{37},\ M_{38}} I_{A1}}, \quad and \ \ g_{mB1} = \sqrt{\mu_n C_{ox} \left(\frac{W}{L}\right)_{M_{41},\ M_{42}} I_{B1}} \quad (2)$$

The aspect ratios used for transistors of Fig. 2 are given in Table 1, and the performance parameters of FD-CCCTA are shown in Table 2.

Table 1: Aspect ratios of MOS Transistors of Fig. 2.

MOS Transistors	W(μm)/L(μm)
$M_{1\text{-}6}$	4.5/0.36
$M_{7,\ 8,\ 9,\ 13}$	36/0.36
$M_{10,\ 11,\ 12,\ 24}$	9/0.36
$M_{14,\ 15,\ 18,\ 19,\ 25,\ 29,\ 30,\ 33,\ 34}$	18/0.18
$M_{16,\ 17,\ 20,\ 21,\ 26,\ 31,\ 32,\ 35,\ 36}$	4.5/0.18
$M_{22,\ 23,\ 27,\ 28}$	0.36/0.36
$M_{37\text{-}44}$	10.8/0.36

Table 2: Performance parameters of FD-CCCTA.

Performance Parameters	Value
Supply Voltage	± 1.2 V
Power Consumption	1.9 mW
Parasitics at Y port (R_Y, C_Y)	2.131 MΩ
Parasitics at X port (R_X)	38.52 Ω
Parasitics at ZA port (R_{ZA}, C_{ZA})	1.22 MΩ, 28 fF
Parasitics at ZB port (R_{ZB}, C_{ZB})	4.4 MΩ, 12 fF
Parasitics at O_1 port (R_{O1}, C_{O1})	2.54 MΩ, 3.42 fF
Parasitics at O_2 port (R_{O2}, C_{O2})	2.3 MΩ, 3.24 fF
Linear variation of I_Z over IX	380 μA to 500 μA
Linear variation of V_X over V_Y	-1.04 V to 1.04 V
Bandwidth of I_Z/I_X	1.4 GHz
Bandwidth of I_{O1}/I_X	73.1 MHz
Bandwidth of I_{O2}/I_X	73.1 MHz

It may be noted in the following section that the mixed-mode filter uses one FD-CCCTA; however, its extended shadow filter uses two FD-CCCTAs. Hence to distinguish the similar mathematical and non-mathematical symbols concerning both the blocks in the shadow filter, superscripts (1) and (2) have been used throughout the paper, such as $g_{mA1}^{(1)}$ and $g_{mB1}^{(1)}$ for the first FD-CCCTA and $g_{mA1}^{(2)}$ and $g_{mB1}^{(2)}$ for second FD-CCCTA.

3 Proposed circuit configuration

The mixed-mode universal filter (also called non-shadow filter) is presented in section 3.1, followed by section 3.2, wherein two mixed-mode shadow filters are discussed.

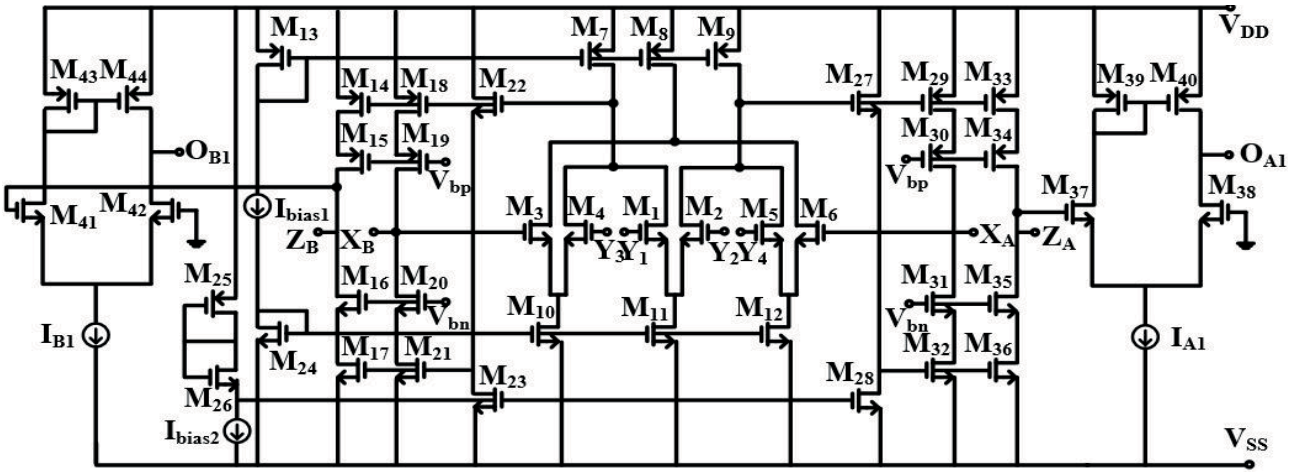

Figure 2: The CMOS-based internal structure of FD-CCCTA.

3.1 Mixed-mode universal filter

The proposed mixed-mode universal filter, depicted in Fig. 3, consists of one FD-CCCTA, three capacitors, and one resistor. The FD-CCCTA being used in the filter is shown in Fig. 2 with the introduction of additional terminals such as $O_{B1c}^{(1)}$, $O_{B1cc}^{(1)}$, and $O_{B1ccc}^{(1)}$, which are copy terminals of the $O_{B1}^{(1)}$. The $O_{B2}^{(1)}$ and $O_{B3}^{(1)}$ are the outputs of the other TAs. These TAs are connected in the cascaded, such as the input of the first TA is connected to the $Z_B^{(1)}$ terminal to get the $O_{B1}^{(1)}$, the input of the second TA is connected to the $O_{B1}^{(1)}$ terminal to get the $O_{B2}^{(1)}$, and similarly, the $O_{B3}^{(1)}$ terminal is obtained. The $-O_{B1}^{(1)}$ and $-O_{B2}^{(1)}$ are 180 degrees phase-shifted of $O_{B1}^{(1)}$ and $O_{B2}^{(1)}$, respectively. At the same time, $O_{B2c}^{(1)}$ and $-O_{B2c}^{(1)}$ are the copies of the $O_{B2}^{(1)}$ and $-O_{B2}^{(1)}$, respectively. Similarly, $O_{B3c}^{(1)}$ and $O_{B3cc}^{(1)}$ are the copies of the $O_{B3}^{(1)}$, while $-O_{B3}^{(1)}$ is 180-degree phase-shifted to $O_{B3}^{(1)}$. Thus, for obtaining the transfer functions in all four modes, such as VM, CM, TAM, and TIM, two input currents, $I_{in1} = I_{in2} = I_{in}$, are used, and a resistor (R_{in}) is used for TAM and TIM.

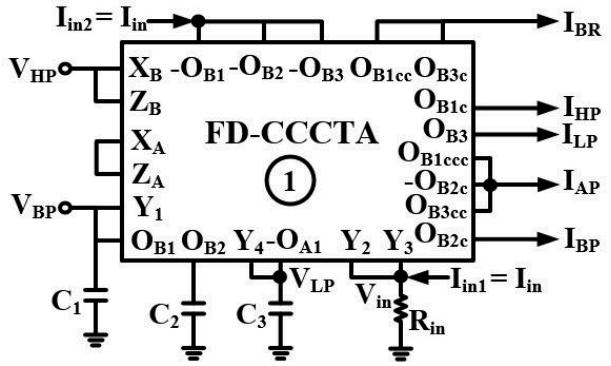

Figure 3: Proposed mixed-mode universal filter.

The routine analysis of the circuit in Fig. 3 results in the following transfers functions:

Voltage Mode (VM) [with $I_{in1} = I_{in2} = 0$, $R_{in} = \infty$ (i.e. Removed)]:

$$\frac{V_{LP}}{V_{in}} = -\frac{g_{mA1}^{(1)} g_{mB1}^{(1)}}{D(s)} \tag{3}$$

$$\frac{V_{BP}}{V_{in}} = \frac{sC_3 g_{mB1}^{(1)}}{D(s)} \tag{4}$$

$$\frac{V_{HP}}{V_{in}} = \frac{s^2 C_1 C_3}{D(s)} \tag{5}$$

The addition of $-V_{HP}$ and V_{LP} results in V_{BR}, while the addition of $-V_{HP}$, V_{BP}, and V_{LP} results in the V_{AP} using another voltage summer (not shown).

$$\frac{V_{BR}}{V_{in}} = -\frac{\left(s^2 C_1 C_3 + g_{mA1}^{(1)} g_{mB1}^{(1)}\right)}{D(s)} \tag{6}$$

$$\frac{V_{AP}}{V_{in}} = -\frac{\left(s^2 C_1 C_3 - sC_3 g_{mB1}^{(1)} + g_{mA1}^{(1)} g_{mB1}^{(1)}\right)}{D(s)} \tag{7}$$

Transimpedance Mode (TIM) [with $V_{in} = 0$, $I_{in2} = 0$]:

$$\frac{V_{LP}}{I_{in}} = -\frac{g_{mA1}^{(1)} g_{mB1}^{(1)} R_{in}}{D(s)} \tag{8}$$

$$\frac{V_{BP}}{I_{in}} = \frac{sC_3 g_{mB1}^{(1)} R_{in}}{D(s)} \tag{9}$$

$$\frac{V_{HP}}{I_{in}} = \frac{s^2 C_1 C_3 R_{in}}{D(s)} \tag{10}$$

The addition of $-V_{HP}$ and V_{LP} results in V_{BR}, while the addition of $-V_{HP}$, V_{BP}, and V_{LP} results in the V_{AP} using another voltage summer (not shown) as follows:

$$\frac{V_{BR}}{I_{in}} = -\frac{\left(s^2 C_1 C_3 + g_{mA1}^{(1)} g_{mB1}^{(1)}\right) R_{in}}{D(s)} \tag{11}$$

$$\frac{V_{AP}}{I_{in}} = -\frac{\left(s^2 C_1 C_3 - sC_3 g_{mB1}^{(1)} + g_{mA1}^{(1)} g_{mB1}^{(1)}\right) R_{in}}{D(s)} \tag{12}$$

Where,

$$D(s) = s^2 C_1 C_3 + sC_3 g_{mB1}^{(1)} + g_{mA1}^{(1)} g_{mB1}^{(1)} \tag{13}$$

The pole frequency (ω_o), quality factor (Q_o) and bandwidth (BW) are:

$$\omega_o = \sqrt{\frac{g_{mA1}^{(1)} g_{mB1}^{(1)}}{C_1 C_3}}, \quad Q_o = \sqrt{\frac{C_1 g_{mB3}^{(1)}}{C_3 g_{mB2}^{(1)}}} \quad and\ BW = \frac{g_{mB2}^{(1)}}{C_1} \tag{14}$$

The sensitivity analysis of ω_o, Q_o and BW using (14) results in:

$$S^{\omega_o}_{g^{(1)}_{mA1}} = S^{\omega_o}_{g^{(1)}_{mB1}} = \frac{1}{2}, S^{\omega_o}_{C_1} = S^{\omega_o}_{C_3} = -\frac{1}{2}$$

$$S^{Q_o}_{g^{(1)}_{mB3}} = S^{Q_o}_{C_1} = \frac{1}{2}, S^{Q_o}_{g^{(1)}_{mB2}} = S^{Q_o}_{C_3} = -\frac{1}{2}$$

$$S^{BW}_{g^{(1)}_{mB2}} = 1, S^{BW}_{C_1} = -1$$

Current Mode (CM) [with $V_{in} = 0$, $I_{in1} = 0$, $R_{in} = 0$]:

$$\frac{I_{LP}}{I_{in}} = \frac{g^{(1)}_{mB2} g^{(1)}_{mB3}}{D(s)} \tag{15}$$

$$\frac{I_{BP}}{I_{in}} = \frac{sC_2 g^{(1)}_{mB2}}{D(s)} \tag{16}$$

$$\frac{I_{HP}}{I_{in}} = \frac{s^2 C_1 C_2}{D(s)} \tag{17}$$

$$\frac{I_{BR}}{I_{in}} = \frac{s^2 C_1 C_2 + g^{(1)}_{mB2} g^{(1)}_{mB3}}{D(s)} \tag{18}$$

$$\frac{I_{AP}}{I_{in}} = \frac{s^2 C_1 C_2 - sC_2 g^{(1)}_{mB2} + g^{(1)}_{mB2} g^{(1)}_{mB3}}{D(s)} \tag{19}$$

Transadmittance Mode (TAM) [with $I_{in1} = 0$]:

$$\frac{I_{LP}}{V_{in}} = \frac{g^{(1)}_{mB2} g^{(1)}_{mB3}}{D(s) * R_{in}} \tag{20}$$

$$\frac{I_{BP}}{V_{in}} = \frac{sC_2 g^{(1)}_{mB2}}{D(s) * R_{in}} \tag{21}$$

$$\frac{I_{HP}}{V_{in}} = \frac{s^2 C_1 C_2}{D(s) * R_{in}} \tag{22}$$

$$\frac{I_{BR}}{V_{in}} = \frac{s^2 C_1 C_2 + g^{(1)}_{mB2} g^{(1)}_{mB3}}{D(s) * R_{in}} \tag{23}$$

$$\frac{I_{AP}}{V_{in}} = \frac{s^2 C_1 C_2 - sC_2 g^{(1)}_{mB2} + g^{(1)}_{mB2} g^{(1)}_{mB3}}{D(s) * R_{in}} \tag{24}$$

Where,

$$D(s) = s^2 C_1 C_2 + sC_2 g^{(1)}_{mB2} + g^{(1)}_{mB2} g^{(1)}_{mB3} \tag{25}$$

The pole frequency (ω_o), quality factor (Q_o) and bandwidth (BW) are:

$$\omega_o = \sqrt{\frac{g^{(1)}_{mB2} g^{(1)}_{mB3}}{C_1 C_2}}, \quad Q_o = \sqrt{\frac{C_1 g^{(1)}_{mB3}}{C_2 g^{(1)}_{mB2}}} \tag{26}$$

$$and\ BW = \frac{g^{(1)}_{mB2}}{C_1}$$

The sensitivity analysis of ω_o, Q_o and BW using (26) results in:

$$S^{\omega_o}_{g^{(1)}_{mB2}} = S^{\omega_o}_{g^{(1)}_{mB3}} = \frac{1}{2}, S^{\omega_o}_{C_1} = S^{\omega_o}_{C_2} = -\frac{1}{2},$$

$$S^{Q_o}_{g^{(1)}_{mB3}} = S^{Q_o}_{C_1} = \frac{1}{2}, S^{Q_o}_{g^{(1)}_{mB2}} = S^{Q_o}_{C_2} = -\frac{1}{2}$$

$$S^{BW}_{g^{(1)}_{mB2}} = 1, S^{BW}_{C_1} = -1$$

The above equation indicates that the ω_o, Q_o, and BW are electronically tunable by bias currents because of $g^{(1)}_{mB2}$ and $g^{(1)}_{mB3}$. Sensitivity of the parameters of eqn. (26) are found within the unity.

3.2 Mixed-mode shadow Filter

Shadow filter also known as frequency agile filter, a recently introduced filters is shown in Fig. 4 [31]. The inclusion of an additional external amplifier in the feedback of the basic filter gives the structure of shadow filter. The introduction of gain (A) of this external amplifier in the filter parameters improves the tunability and eases in frequency agility in comparison of the conventional tuning technique.

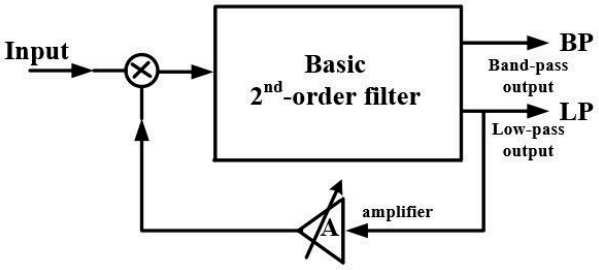

Figure 4: Scheme of the shadow filter [31].

In line with Fig. 4, block diagram for the implementation of mixed-mode shadow filter is shown in Fig. 5. Combination of voltage and current signals at the input as well as at the output form all the modes such as VM, CM, TIM, and TAM. Two amplifiers with gains A_1 and A_2 multiplied with the V_{AP} and I_{BP} are fed-back to the voltage and current input signals, respectively.

In this section, two topologies are proposed for mixed-mode shadow filters using basic mixed mode UF of Fig. 3. The first topology realizes VM and CM universal filters, and the second topology realizes all four modes of

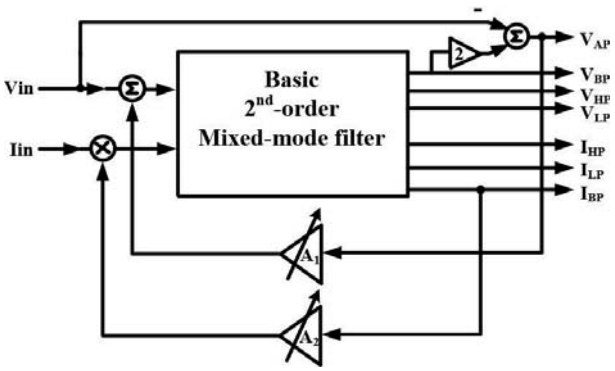

Figure 5: Block diagram for the implementation of mixed-mode shadow filter.

mixed-mode filters. Both the topologies have been implemented on the basis of the structure shown in Fig. 5.

3.2.1 First shadow filter (VM and CM)

The proposed shadow filter in the VM and CM, as shown in Fig. 6, consists of the above mixed-mode universal filter of Fig. 3 along with a second FD-CCCTA block and two variable resistors (R_1 & R_2) consisting of MOSs. V_{BP} is given to $Y_2^{(2)}$ and $Y_4^{(2)}$ terminals for the sake of the VM shadow filter, and I_{BP} is given to the $X_A^{(2)}$ terminal for the CM shadow filter. The second FD-CCCTA in Fig. 6 aims to create two amplifiers, A_1 and A_2, in the feedback loop [32] of the previous mixed-mode filter (Fig. 3) to obtain the VM and CM shadow filters. By routine analysis of Fig. 6, it is shown in eqn. (38) that

$$A_1 = g_{mB}^{(2)} R_1 \text{ and } A_2 = g_{mA}^{(2)} R_2$$

The value of MOS resistors can be adjusted with their respective bias voltages, V_{C1} and V_{C2} [33]. The equation for the resistance is:

$$R = \frac{L}{2\mu C_{ox} W\left(V_{Ci} - V_T\right)} \tag{27}$$

Where L and W are the channel length and channel width, μ is the effective mobility, C_{ox} is the gate oxide capacitance, and V_T is the threshold voltage of the MOS transistor.

The routine analysis of the circuit Fig. 6 results in the following transfer function:

The port relationships of FD-CCCTA suggests:

$$\begin{aligned} &V_{XA} = V_{Y1} - V_{Y2} + V_{Y3} \\ &and\, V_{XB} = -V_{Y1} + V_{Y2} + V_{Y4} \end{aligned} \tag{28}$$

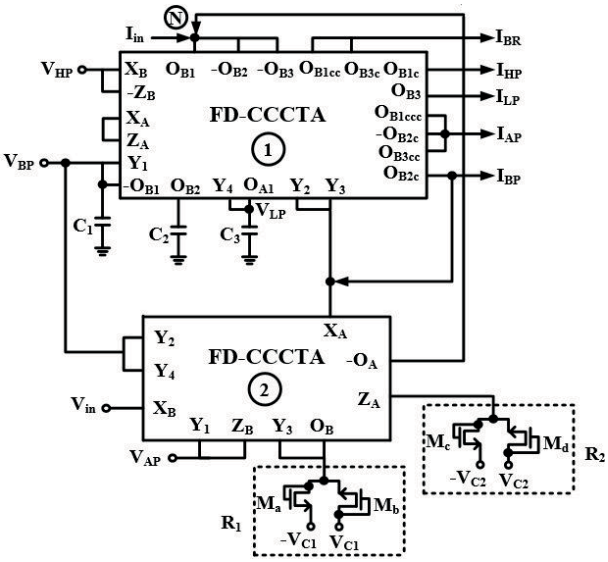

Figure 6: Proposed first shadow filter.

Therefore for FD-CCCTA-1, we get:

$$V_{XA}^{(1)} = V_{BP} \tag{29}$$

$$V_{HP} = -V_{BP} + V_{Y2}^{(1)} + V_{LP} \tag{30}$$

While for FD-CCCTA-2 we get:

$$V_{XA}^{(2)} = V_{AP} - V_{BP} + V_{Y3}^{(2)} \tag{31}$$

$$V_{in} = -V_{AP} + 2V_{BP} \tag{32}$$

Again, the port relationships of FD-CCCTA-1 results:

$$I_{OA1}^{(1)} = g_{mA1}^{(1)} V_{ZA} \; and \; I_{OB1}^{(1)} = g_{mB1}^{(1)} V_{ZB} \tag{33}$$

Which corresponds to:

$$V_{LP} sC_3 = g_{mA1}^{(1)} V_{BP} \; and - V_{BP} sC_1 = g_{mB1}^{(1)} V_{HP} \tag{34}$$

Another port relationships of FD-CCCTA-1 results:

$$I_{OB2}^{(1)} = g_{mB2}^{(1)} V_{OB1} \; and \; I_{OB3}^{(1)} = g_{mB3}^{(1)} V_{OB2} \tag{35}$$

Which corresponds:

$$I_{BP} = -g_{mB2}^{(1)} \frac{I_{HP}}{sC_1} and \; I_{LP} = g_{mB3}^{(1)} \frac{I_{BP}}{sC_2} \tag{36}$$

Whereas, port relationships of FD-CCCTA-2 results:

$$I_{-OA}^{(2)} = -g_{mA}^{(2)} V_{ZA} \; and \; I_{OB}^{(2)} = g_{mB}^{(2)} V_{ZB} \tag{37}$$

Hence, (35) results:

$$I_{-OA}^{(2)} = -g_{mA}^{(2)} R_2 I_{BP} \; and \; \frac{V_{Y3}^{(2)}}{R_1} = g_{mB}^{(2)} V_{AP} \tag{38}$$

It can be written as:

$$I_{-OA}^{(2)} = -A_2 I_{BP} \; and \; V_{Y3}^{(2)} = A_1 V_{AP} \tag{39}$$

Where $A_1 = g_{mB}^{(2)} R_1$ and $A_2 = g_{mA}^{(2)} R_2$ (40)

Eqn. (31) can be rewritten after substituting the value of

$V_{Y3}^{(2)}$ from (39) as

$$V_{XA}^{(2)} = V_{AP}\left(1 + A_1\right) - V_{BP} \tag{41}$$

Now, (28) can be rewritten as:

$$V_{HP} = -V_{BP} + V_{XA}^{(2)} + V_{LP} \tag{42}$$

Therefore,

$$V_{HP} = -V_{BP} + V_{AP}\left(1 + A_1\right) - V_{BP} + V_{LP} \tag{43}$$

Substituting the value of V_{AP} from eqn. (32) into eqn. (43) gives:

$$V_{in}\left(1 + A_1\right) = -V_{HP} + 2V_{BP} A_1 + V_{LP} \tag{44}$$

Whereas for the current mode (CM), the expression of currents at node N is given as:

$$I_{in} = -I_{HP} + I_{BP}\left(1 + A_2\right) + I_{LP} \tag{45}$$

Now the voltage mode transfer functions are obtained by using eqn. (34) and eqn. (44) while, current mode transfer functions are obtained by using eqn. (36) and eqn. (45) as follows:

Voltage mode [with Iin = 0]:

$$\frac{V_{LP}}{V_{in}} = \frac{g_{mA1}^{(1)} g_{mB1}^{(1)}\left(1 + A_1\right)}{D(s)} \tag{46}$$

$$\frac{V_{BP}}{V_{in}} = \frac{sC_3 g_{mB1}^{(1)}\left(1 + A_1\right)}{D(s)} \tag{47}$$

$$\frac{V_{HP}}{V_{in}} = -\frac{s^2 C_1 C_3\left(1 + A_1\right)}{D(s)} \tag{48}$$

$$\frac{V_{AP}}{V_{in}} = -\frac{\left(s^2 C_1 C_3 - 2sC_3 g_{mB1}^{(1)} + g_{mA1}^{(1)} g_{mB1}^{(1)}\right)}{D(s)} \tag{49}$$

By the addition of -V_{HP} and V_{LP} results into V_{BR} using voltage summer.

$$\frac{V_{BR}}{V_{in}} = \frac{\left(s^2 C_1 C_3 + g_{mA1}^{(1)} g_{mB1}^{(1)}\right)\left(1 + A_1\right)}{D(s)} \tag{50}$$

Where,

$$\begin{aligned} A_1 &= g_{mB}^{(2)} R_1 \\ D(s) &= s^2 C_1 C_3 + 2A_1 sC_3 g_{mB1}^{(1)} + g_{mA1}^{(1)} g_{mB1}^{(1)} \end{aligned} \tag{51}$$

The pole frequency (ω_o), quality factor (Q_o) and bandwidth (BW) are:

$$\begin{aligned} &\omega_o = \sqrt{\frac{g_{mA1}^{(1)} g_{mB1}^{(1)}}{C_1 C_3}}, \quad Q_o = \frac{1}{2A_1}\sqrt{\frac{C_1 g_{mA1}^{(1)}}{C_3 g_{mB1}^{(1)}}} \\ &and \; BW = 2A_1 \frac{g_{mB1}^{(1)}}{C_1} \end{aligned} \tag{52}$$

Considering $C_1 = C_3$, eqn. (52) gives:

$$\begin{aligned} &\omega_o = \frac{\sqrt{g_{mA1}^{(1)} g_{mB1}^{(1)}}}{C}, \quad Q_o = \frac{1}{2A_1}\sqrt{\frac{g_{mA1}^{(1)}}{g_{mB1}^{(1)}}} \\ &and \; BW = 2A_1 \frac{g_{mB1}^{(1)}}{C} \end{aligned} \tag{53}$$

The gain of the filter can be expressed as:

$$\begin{aligned} &A_{LP} = A_{HP} = A_{BR} = \left(1 + A_1\right), A_{BP} = \frac{\left(1 + A_1\right)}{2A_1}, \\ &A_{AP} = \frac{1}{A_1} \end{aligned} \tag{54}$$

The sensitivity analysis of ω_o, Q_o and BW using (52) results in:

$$S_{g_{mA1}^{(1)}}^{\omega_o} = S_{g_{mB1}^{(1)}}^{\omega_o} = \frac{1}{2}, S_{C_1}^{\omega_o} = S_{C_3}^{\omega_o} = -\frac{1}{2},$$

$$S_{g_{mA1}^{(1)}}^{Q_o} = S_{C_1}^{Q_o} = \frac{1}{2}, S_{g_{mB1}^{(1)}}^{Q_o} = S_{C_3}^{Q_o} = -\frac{1}{2},$$

$$S_{g_{mB}^{(2)}}^{Q_o} = S_{R_1}^{Q_o} = -$$

$$S_{g_{mB1}^{(1)}}^{BW} = 1, S_{C_1}^{BW} = -1, S_{g_{mB}^{(2)}}^{BW} = S_{R_1}^{BW} = 1$$

The above eqn. (53) indicates that the ω_o, Q_o, and BW are electronically tunable by bias currents because of

$g_{mA1}^{(1)}$, and $g_{mB1}^{(1)}$, and ω_o is independently tunable by C, while Q_o is independently tunable by gain A_1, i.e., $g_{mB}^{(2)}$ as well as R_1. Also, the tuning of gain is obtained by A_1.

Current mode [with Vin = 0]:

$$\frac{I_{LP}}{I_{in}} = \frac{g_{mB2}^{(1)} g_{mB3}^{(1)}}{D(s)} \tag{55}$$

$$\frac{I_{BP}}{I_{in}} = \frac{sC_2 g_{mB2}^{(1)}}{D(s)} \tag{56}$$

$$\frac{I_{HP}}{I_{in}} = -\frac{s^2 C_1 C_2}{D(s)} \tag{57}$$

$$\frac{I_{BR}}{I_{in}} = \frac{s^2 C_1 C_2 + g_{mB2}^{(1)} g_{mB3}^{(1)}}{D(s)} \tag{58}$$

$$\frac{I_{AP}}{I_{in}} = \frac{\left(s^2 C_1 C_2 - sC_2 g_{mB2}^{(1)} + g_{mB2}^{(1)} g_{mB3}^{(1)}\right)}{D(s)} \tag{59}$$

Where,

$$D(s) = s^2 C_1 C_2 + (1 + A_2) sC_2 g_{mB2}^{(1)} + g_{mB2}^{(1)} g_{mB3}^{(1)}$$
$$and\ A_2 = g_{mA}^{(2)} R_2 \tag{60}$$

The pole frequency (ω_o), quality factor (Q_o) and bandwidth (BW) are:

$$\omega_o = \sqrt{\frac{g_{mB2}^{(1)} g_{mB3}^{(1)}}{C_1 C_2}}, \quad Q_o = \frac{1}{(1 + A_2)} \sqrt{\frac{C_1 g_{mB3}^{(1)}}{C_2 g_{mB2}^{(1)}}}$$
$$and\ BW = (1 + A_2) \frac{g_{mB2}^{(1)}}{C_1} \tag{61}$$

Considering, $C_1 = C_2$, eqn. (61) gives:

$$\omega_o = \frac{\sqrt{g_{mB2}^{(1)} g_{mB3}^{(1)}}}{C}, \quad Q_o = \frac{1}{(1 + A_2)} \sqrt{\frac{g_{mB3}^{(1)}}{g_{mB2}^{(1)}}}$$
$$and\ BW = (1 + A_2) \frac{g_{mB2}^{(1)}}{C} \tag{62}$$

The sensitivity analysis of ω_o, Q_o and BW using (61) results in:

$$S_{g_{mB2}^{(1)}}^{\omega_o} = S_{g_{mB3}^{(1)}}^{\omega_o} = \frac{1}{2}, S_{C_1}^{\omega_o} = S_{C_2}^{\omega_o} = -\frac{1}{2},$$

$$S_{g_{mB3}^{(1)}}^{Q_o} = S_{C_1}^{Q_o} = \frac{1}{2}, S_{g_{mB2}^{(1)}}^{Q_o} = S_{C_2}^{Q_o} = -\frac{1}{2},$$

$$S_{g_{mA}^{(2)}}^{Q_o} = S_{R_2}^{Q_o} = -\frac{A_2}{1 + A_2}$$

$$S_{g_{mB2}^{(1)}}^{BW} = 1, S_{C_1}^{BW} = -1, S_{g_{mA}^{(2)}}^{BW} = S_{R_2}^{BW} = \frac{A_2}{1 + A_2}$$

The above equation indicates that the ω_o, Q_o, and BW are electronically tunable by bias currents because of $g_{mB2}^{(1)}$, and $g_{mB3}^{(1)}$, and ω_o is independently tunable by C, while Q_o is independently tunable by gain A_2, i.e., $g_{mA}^{(2)}$ as well as R_2. Sensitivity analysis of all the parameters resulted within the unity.

3.2.2 Second shadow filter (all four modes)

The second shadow filter shown in Fig. 7 realizes all the modes, such as VM, CM, TAM, and TIM. This circuit is a slight alteration of Fig. 6 with the addition of one input resistor (R_{in}) and one more input current such that $I_{in1} = I_{in2} = I_{in}$.

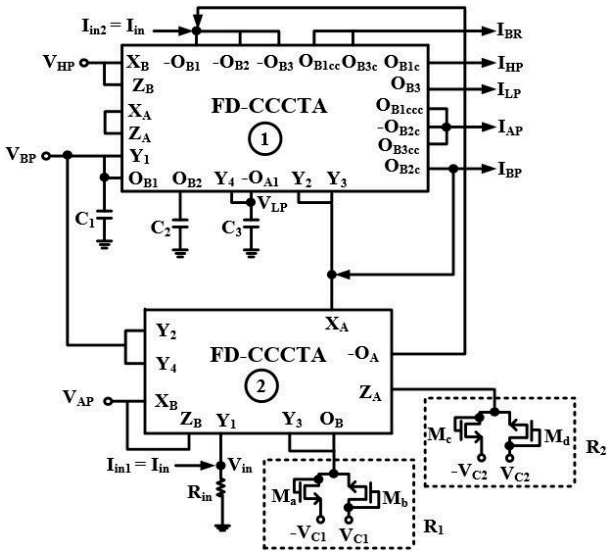

Figure 7: Proposed second mixed mode shadow filter.

The routine analysis of the circuit Fig. 7 in line with Fig. 6 results in the following transfer functions for VM, CM, TIM, and TAM:

Voltage mode (VM) [with $I_{in1} = I_{in2} = 0$, $R_{in} = \infty$ (Removed)]:

$$\frac{V_{LP}}{V_{in}} = -\frac{g_{mA1}^{(1)} g_{mB1}^{(1)} (1 - A_1)}{D(s)} \tag{63}$$

$$\frac{V_{BP}}{V_{in}} = \frac{sC_3 g_{mB1}^{(1)}\left(1-A_1\right)}{D(s)} \quad (64)$$

$$\frac{V_{HP}}{V_{in}} = \frac{s^2 C_1 C_3 \left(1-A_1\right)}{D(s)} \quad (65)$$

$$\frac{V_{AP}}{V_{in}} = -\frac{\left(s^2 C_1 C_3 - sC_3 g_{mB1}^{(1)} + g_{mA1}^{(1)} g_{mB1}^{(1)}\right)}{D(s)} \quad (66)$$

By the addition of V_{HP} and $-V_{LP}$ results into V_{BR} using voltage summer.

$$\frac{V_{BR}}{V_{in}} = \frac{\left(s^2 C_1 C_3 + g_{mA1}^{(1)} g_{mB1}^{(1)}\right)\left(1-A_1\right)}{D(s)} \quad (67)$$

Transimpedance mode (TIM) [with $V_{in} = 0$, $I_{in2} = 0$]:

$$\frac{V_{LP}}{I_{in}} = -\frac{g_{mA1}^{(1)} g_{mB1}^{(1)} R_{in}\left(1-A_1\right)}{D(s)} \quad (68)$$

$$\frac{V_{BP}}{I_{in}} = \frac{sC_3 g_{mB1}^{(1)} R_{in}\left(1-A_1\right)}{D(s)} \quad (69)$$

$$\frac{V_{HP}}{I_{in}} = \frac{s^2 C_1 C_3 R_{in}\left(1-A_1\right)}{D(s)} \quad (70)$$

$$\frac{V_{AP}}{I_{in}} = -\frac{\left(s^2 C_1 C_3 - sC_3 g_{mB1}^{(1)} + g_{mA1}^{(1)} g_{mB1}^{(1)}\right) R_{in}}{D(s)} \quad (71)$$

By the addition of V_{HP} and $-V_{LP}$ results into V_{BR} using voltage summer.

$$\frac{V_{BR}}{I_{in}} = \frac{\left(s^2 C_1 C_3 + g_{mA1}^{(1)} g_{mB1}^{(1)}\right) R_{in}\left(1-A_1\right)}{D(s)} \quad (72)$$

Where,

$$D(s) = s^2 C_1 C_3 + 2\left(1-A_1\right) sC_3 g_{mB1}^{(1)} + g_{mA1}^{(1)} g_{mB1}^{(1)}$$
$$and\ A_1 = g_{mB}^{(2)} R_1 \quad (73)$$

The pole frequency (ω_o), quality factor (Q_o) and bandwidth (BW) are:

$$\omega_o = \sqrt{\frac{g_{mA1}^{(1)} g_{mB1}^{(1)}}{C_1 C_3}}, \quad Q_o = \frac{1}{2\left(1-A_1\right)}\sqrt{\frac{C_1 g_{mA1}^{(1)}}{C_3 g_{mB1}^{(1)}}} \quad (74)$$
$$and\ BW = 2\left(1-A_1\right)\frac{g_{mB1}^{(1)}}{C_1}$$

Considering, $C_1 = C_3$, eqn. (74) gives:

$$\omega_o = \frac{\sqrt{g_{mA1}^{(1)} g_{mB1}^{(1)}}}{C}, \quad Q_o = \frac{1}{2\left(1-A_1\right)}\sqrt{\frac{g_{mA1}^{(1)}}{g_{mB1}^{(1)}}} \quad (75)$$
$$and\ BW = 2\left(1-A_1\right)\frac{g_{mB1}^{(1)}}{C}$$

The gain of the filter can be expressed as:

$$A_{LP} = A_{HP} = A_{BR} = \left(1-A_1\right), A_{BP} = \frac{\left(1-A_1\right)}{2\left(1-A_1\right)},$$
$$and \quad A_{AP} = \frac{1}{2\left(1-A_1\right)} \quad (76)$$

The sensitivity analysis of ω_o, Q_o and BW using (74) results in:

$$S_{g_{mA1}^{(1)}}^{\omega_o} = S_{g_{mB1}^{(1)}}^{\omega_o} = \frac{1}{2}, S_{C_1}^{\omega_o} = S_{C_3}^{\omega_o} = -\frac{1}{2},$$

$$S_{g_{mA1}^{(1)}}^{Q_o} = S_{C_1}^{Q_o} = \frac{1}{2}, S_{g_{mB1}^{(1)}}^{Q_o} = S_{C_3}^{Q_o} = -\frac{1}{2},$$

$$S_{g_{mB}^{(2)}}^{Q_o} = S_{R_1}^{Q_o} = -\frac{\mathrm{A}_1}{1-\mathrm{A}_1}$$

$$S_{g_{mB1}^{(1)}}^{BW} = 1, S_{C_1}^{BW} = -1, S_{g_{mB}^{(2)}}^{BW} = S_{R_1}^{BW} = \frac{\mathrm{A}_1}{1-\mathrm{A}_1}$$

The (73) indicates that the ω_o, Q_o, and BW are electronically tunable by bias currents because of $g_{mA1}^{(1)}$ and $g_{mB1}^{(1)}$. Moreover, ω_o is independently tunable by C, while Q_o is independently tunable by gain A_1, i.e., $g_{mB}^{(2)}$ and R_1. Also, the VM and TIM shadow filter's gain is tunable by A_1 as indicated in (74).

Current mode (CM) [with $V_{in} = 0$, $I_{in1} = 0$, $R_{in} = 0$]:

$$\frac{I_{LP}}{I_{in}} = \frac{g_{mB2}^{(1)} g_{mB3}^{(1)}}{D(s)} \quad (77)$$

$$\frac{I_{BP}}{I_{in}} = \frac{sC_2 g_{mB2}^{(1)}}{D(s)} \quad (78)$$

$$\frac{I_{HP}}{I_{in}} = \frac{s^2 C_1 C_2}{D(s)} \quad (79)$$

$$\frac{I_{BR}}{I_{in}} = \frac{s^2 C_1 C_2 + g_{mB2}^{(1)} g_{mB3}^{(1)}}{D(s)} \quad (80)$$

$$\frac{I_{AP}}{I_{in}} = \frac{\left(s^2C_1C_2 - sC_2g_{mB2}^{(1)} + g_{mB2}^{(1)}g_{mB3}^{(1)}\right)}{D(s)} \quad (81)$$

Transadmittance mode (TAM) [with $I_{in1} = 0$]:

$$\frac{I_{LP}}{V_{in}} = \frac{g_{mB2}^{(1)}g_{mB3}^{(1)}}{D(s)*R_{in}} \quad (82)$$

$$\frac{I_{BP}}{V_{in}} = \frac{sC_2g_{mB2}^{(1)}}{D(s)*R_{in}} \quad (83)$$

$$\frac{I_{HP}}{V_{in}} = \frac{s^2C_1C_2}{D(s)*R_{in}} \quad (84)$$

$$\frac{I_{BR}}{V_{in}} = \frac{s^2C_1C_2 + g_{mB2}^{(1)}g_{mB3}^{(1)}}{D(s)*R_{in}} \quad (85)$$

$$\frac{I_{AP}}{V_{in}} = \frac{\left(s^2C_1C_2 - sC_2g_{mB2}^{(1)} + g_{mB2}^{(1)}g_{mB3}^{(1)}\right)}{D(s)*R_{in}} \quad (86)$$

Where,

$$D(s) = s^2C_1C_2 + (1+A_2)sC_2g_{mB2}^{(1)} + g_{mB2}^{(1)}g_{mB3}^{(1)}$$
$$and\ A_2 = g_{mA}^{(2)}R_2 \quad (87)$$

The pole frequency (ω_o), quality factor (Q_o) and bandwidth (BW) are:

$$\omega_o = \sqrt{\frac{g_{mB2}^{(1)}g_{mB3}^{(1)}}{C_1C_2}}, \quad Q_o = \frac{1}{(1+A_2)}\sqrt{\frac{C_1g_{mB3}^{(1)}}{C_2g_{mB2}^{(1)}}}$$
$$and\ BW = (1+A_2)\frac{g_{mB2}^{(1)}}{C_1} \quad (88)$$

Considering, $C_1 = C_2$, eqn. (88) gives:

$$\omega_o = \frac{\sqrt{g_{mB2}^{(1)}g_{mB3}^{(1)}}}{C},\ Q_o = \frac{1}{(1+A_2)}\sqrt{\frac{g_{mB3}^{(1)}}{g_{mB2}^{(1)}}}$$
$$and\ BW = (1+A_2)\frac{g_{mB2}^{(1)}}{C} \quad (89)$$

The sensitivity analysis of ω_o, Q_o and BW using (88) results in:

$$S_{g_{mB2}^{(1)}}^{\omega_o} = S_{g_{mB3}^{(1)}}^{\omega_o} = \frac{1}{2}, S_{C_1}^{\omega_o} = S_{C_2}^{\omega_o} = -\frac{1}{2},$$

$$S_{g_{mB3}^{(1)}}^{Q_o} = S_{C_1}^{Q_o} = \frac{1}{2}, S_{g_{mB2}^{(1)}}^{Q_o} = S_{C_2}^{Q_o} = -\frac{1}{2},$$

$$S_{g_{mA}^{(2)}}^{Q_o} = S_{R_2}^{Q_o} = -\frac{A_2}{1+A_2}$$

$$S_{g_{mB2}^{(1)}}^{BW} = 1, S_{C_1}^{BW} = -1, S_{g_{mA}^{(2)}}^{BW} = S_{R_2}^{BW} = \frac{A_2}{1+A_2}$$

The equation (89) indicates that the ω_o, Q_o, and BW are electronically tunable by bias currents because of $g_{mB2}^{(1)}$ and $g_{mB3}^{(1)}$. Moreover, ω_o is independently tunable by C, while Q_o is independently tunable by gain A_2, i.e., $g_{mA}^{(2)}$ and R_2. Sensitivity analysis of all the parameters results within the unity magnitude.

4 Non-ideality analysis

Non-ideal transfer gains and active building block parasitics will have an impact practically. Sections 4.1 discusses the effect due to non-ideal transfer gains. and section 4.2 discusses the effect due to parasitics of FD-CCCTA.

4.1 Non-ideal transfer gain of FD-CCCTA

The port relationship is modified as follows when taking into account the non-idealities of the voltage, current, and transconductance gains of FD-CCCTA:

$$\begin{bmatrix} I_{Y1} \\ I_{Y2} \\ I_{Y3} \\ I_{Y4} \\ V_{XA} \\ V_{XB} \\ I_{ZA} \\ I_{ZB} \\ I_{OA1} \\ I_{OB1} \end{bmatrix} = \begin{bmatrix} 0 & 0 & 0 & 0 & 0 & 0 & 0 & 0 & 0 & 0 \\ 0 & 0 & 0 & 0 & 0 & 0 & 0 & 0 & 0 & 0 \\ 0 & 0 & 0 & 0 & 0 & 0 & 0 & 0 & 0 & 0 \\ 0 & 0 & 0 & 0 & 0 & 0 & 0 & 0 & 0 & 0 \\ \beta_{a1} & -\beta_{a2} & \beta_{a3} & 0 & 0 & 0 & 0 & 0 & 0 & 0 \\ -\beta_{b1} & \beta_{b2} & 0 & \beta_{b3} & 0 & 0 & 0 & 0 & 0 & 0 \\ 0 & 0 & 0 & 0 & \alpha_a & 0 & 0 & 0 & 0 & 0 \\ 0 & 0 & 0 & 0 & 0 & \alpha_b & 0 & 0 & 0 & 0 \\ 0 & 0 & 0 & 0 & 0 & 0 & \gamma_{a1}g_{mA1} & 0 & 0 & 0 \\ 0 & 0 & 0 & 0 & 0 & 0 & 0 & \gamma_{b1}g_{mB1} & 0 & 0 \end{bmatrix} \begin{bmatrix} V_{Y1} \\ V_{Y2} \\ V_{Y3} \\ V_{Y4} \\ I_{XA} \\ I_{XB} \\ V_{ZA} \\ V_{ZB} \\ V_{OA1} \\ V_{OB1} \end{bmatrix} \quad (90)$$

Where β_{ai} (i=1,2,3) is the voltage transfer gain between $Y_{(i)}$ and X_A terminals, β_{bi} (i=1,2,3) is the voltage transfer gain between $Y_{(i)}$ and X_B terminals, is the current transfer gain between I_{ZA} and I_{XA} terminals, α_b is the current transfer gain between I_{ZB} and I_{XB} terminals, γ_{a1} is the transconductance gain between I_{OA1} and V_{OA1}, and γ_{b1} is the transconductance gain between I_{OB1} and V_{OB1}. These gain factors are found unity ideally but they deviate slightly from unity practically. The transfer functions of Fig. 3 after considering the non-idealities are obtained as follows:

Voltage Mode (VM):

$$\frac{V_{LP}}{V_{in}} = -\frac{g_{mA1}^{(1)} g_{mB1}^{(1)} \beta_{a1} \beta_{b2} \gamma_{a1} \gamma_{b1}}{D(s)} \quad (91)$$

$$\frac{V_{BP}}{V_{in}} = \frac{sC_3 g_{mB1}^{(1)} \beta_{b2} \gamma_{B1}}{D(s)} \quad (92)$$

$$\frac{V_{HP}}{V_{in}} = \frac{s^2 C_1 C_3 \beta_{b2}}{D(s)} \quad (93)$$

$$\frac{V_{BR}}{V_{in}} = -\frac{\left(s^2 C_1 C_3 \beta_{b2} + g_{mA1}^{(1)} g_{mB1}^{(1)} \beta_{a1} \beta_{b2} \gamma_{a1} \gamma_{b1}\right)}{D(s)} \quad (94)$$

$$\frac{V_{AP}}{V_{in}} = -\frac{\begin{pmatrix} s^2 C_1 C_3 \beta_{b2} - sC_3 g_{mB1}^{(1)} \beta_{b2} \gamma_{B1} \\ + g_{mA1}^{(1)} g_{mB1}^{(1)} \beta_{a1} \beta_{b2} \gamma_{a1} \gamma_{b1} \end{pmatrix}}{D(s)} \quad (95)$$

Transimpedance Mode (TIM):

$$\frac{V_{LP}}{I_{in}} = -\frac{g_{mA1}^{(1)} g_{mB1}^{(1)} \beta_{a1} \beta_{b2} \gamma_{a1} \gamma_{b1} R_{in}}{D(s)} \quad (96)$$

$$\frac{V_{BP}}{I_{in}} = \frac{sC_3 g_{mB1}^{(1)} \beta_{b2} \gamma_{b1} R_{in}}{D(s)} \quad (97)$$

$$\frac{V_{HP}}{I_{in}} = \frac{s^2 C_1 C_3 \beta_{b2} R_{in}}{D(s)} \quad (98)$$

$$\frac{V_{BR}}{I_{in}} = -\frac{\begin{pmatrix} s^2 C_1 C_3 \beta_{b2} \\ + g_{mA1}^{(1)} g_{mB1}^{(1)} \beta_{a1} \beta_{b2} \gamma_{a1} \gamma_{b1} \end{pmatrix} R_{in}}{D(s)} \quad (99)$$

$$\frac{V_{AP}}{I_{in}} = -\frac{\begin{pmatrix} s^2 C_1 C_3 \beta_{b2} - sC_3 g_{mB1}^{(1)} \beta_{b2} \gamma_{b1} \\ + g_{mA1}^{(1)} g_{mB1}^{(1)} \beta_{a1} \beta_{b2} \gamma_{a1} \gamma_{b1} \end{pmatrix} R_{in}}{D(s)} \quad (100)$$

Where,

$$D(s) = s^2 C_1 C_3 + sC_3 g_{mB1}^{(1)} \beta_{a1} \gamma_{b1} + g_{mA1}^{(1)} g_{mB1}^{(1)} \beta_{a1} \beta_{b2} \gamma_{a1} \gamma_{b1} \quad (101)$$

The pole frequency (ω_o), quality factor (Q_o) and bandwidth (BW) are:

$$\omega_o = \sqrt{\frac{g_{mA1}^{(1)} g_{mB1}^{(1)} \beta_{a1} \beta_{b2} \gamma_{a1} \gamma_{b1}}{C_1 C_3}}, Q_o = \sqrt{\frac{C_1 g_{mA1}^{(1)} \beta_{b2} \gamma_{a1}}{C_3 g_{mB1}^{(1)} \beta_{a1} \gamma_{b1}}} \quad (102)$$

$$and\ BW = \frac{g_{mB1}^{(1)} \beta_{a1} \gamma_{b1}}{C_1}$$

Current Mode (CM):

$$\frac{I_{LP}}{I_{in}} = \frac{g_{mB2}^{(1)} g_{mB3}^{(1)} \gamma_{b2} \gamma_{b3}}{D(s)} \quad (103)$$

$$\frac{I_{BP}}{I_{in}} = \frac{sC_2 g_{mB2}^{(1)} \gamma_{b2}}{D(s)} \quad (104)$$

$$\frac{I_{HP}}{I_{in}} = \frac{s^2 C_1 C_2}{D(s)} \quad (105)$$

$$\frac{I_{BR}}{I_{in}} = \frac{s^2 C_1 C_2 + g_{mB2}^{(1)} g_{mB3}^{(1)} \gamma_{b2} \gamma_{b3}}{D(s)} \quad (106)$$

$$\frac{I_{AP}}{I_{in}} = \frac{\begin{matrix} s^2 C_1 C_2 - sC_2 g_{mB2}^{(1)} \gamma_{b2} \\ + g_{mB2}^{(1)} g_{mB3}^{(1)} \gamma_{b2} \gamma_{b3} \end{matrix}}{D(s)} \quad (107)$$

Transadmittance Mode (TAM) [with $I_{in1} = 0$]:

$$\frac{I_{LP}}{V_{in}} = \frac{g_{mB2}^{(1)} g_{mB3}^{(1)} \gamma_{b2} \gamma_{b3}}{D(s) R_{in}} \quad (108)$$

$$\frac{I_{BP}}{V_{in}} = \frac{sC_2 g_{mB2}^{(1)} \gamma_{b2}}{D(s) R_{in}} \quad (109)$$

$$\frac{I_{HP}}{V_{in}} = \frac{s^2 C_1 C_2}{D(s) R_{in}} \quad (110)$$

$$\frac{I_{BR}}{V_{in}} = \frac{s^2 C_1 C_2 + g_{mB2}^{(1)} g_{mB3}^{(1)} \gamma_{b2} \gamma_{b3}}{D(s) R_{in}} \quad (111)$$

$$\frac{I_{AP}}{V_{in}} = \frac{\begin{matrix} s^2 C_1 C_2 - sC_2 g_{mB2}^{(1)} \gamma_{b2} \\ + g_{mB2}^{(1)} g_{mB3}^{(1)} \gamma_{b2} \gamma_{b3} \end{matrix}}{D(s) R_{in}} \quad (112)$$

Where,

$$D(s) = s^2 C_1 C_2 + sC_2 g_{mB2}^{(1)} \gamma_{b2} + g_{mB2}^{(1)} g_{mB3}^{(1)} \gamma_{b2} \gamma_{b3} \quad (113)$$

The pole frequency (ω_o), quality factor (Q_o) and bandwidth (BW) are:

$$\omega_o = \sqrt{\frac{g_{mB2}^{(1)} g_{mB3}^{(1)} \gamma_{b2} \gamma_{b3}}{C_1 C_2}}, \quad Q_o = \sqrt{\frac{C_1 g_{mB3}^{(1)} \gamma_{b3}}{C_3 g_{mB2}^{(1)} \gamma_{b2}}} \quad (114)$$

$$and\ BW = \frac{g_{mB2}^{(1)} \gamma_{b2}}{C_1}$$

The transfer functions of Fig. 6 after considering non-idealities result:

Voltage mode:

$$\frac{V_{LP}}{V_{in}}=\frac{g_{mA1}^{(1)}g_{mB1}^{(1)}\left(\beta_{a1}+A_1\beta_{a3}\beta_{b1\gamma_{b1}}\right)\beta_{a1}\beta_{b2}\gamma_{a1}\gamma_{b1}}{D(s)} \quad (115)$$

$$\frac{V_{BP}}{V_{in}}=\frac{sC_3g_{mB1}^{(1)}\beta_{b2}\gamma_{B1}\left(\beta_{a1}+A_1\beta_{a3}\beta_{b1}\gamma_{b1}\right)}{D(s)} \quad (116)$$

$$\frac{V_{HP}}{V_{in}}=-\frac{s^2C_1C_3\beta_{b2}\left(\beta_{a1}+A_1\beta_{a3}\beta_{b1\gamma_{b1}}\right)}{D(s)} \quad (117)$$

$$\frac{V_{AP}}{V_{in}}=-\frac{\begin{pmatrix}s^2C_1C_3\beta_{b2}-sC_3g_{mB1}^{(1)}\beta_{b2}\gamma_{B1}\\+g_{mA1}^{(1)}g_{mB1}^{(1)}\beta_{a1}\beta_{b2}\gamma_{a1}\gamma_{b1}\end{pmatrix}}{D(s)} \quad (118)$$

$$\frac{V_{BR}}{V_{in}}=\frac{\begin{pmatrix}s^2C_1C_3\beta_{b2}\\+g_{mA1}^{(1)}g_{mB1}^{(1)}\beta_{a1}\beta_{b2}\gamma_{a1}\gamma_{b1}\end{pmatrix}\begin{pmatrix}\beta_{a1}\\+A_1\beta_{a3}\beta_{b1\gamma_{b1}}\end{pmatrix}}{D(s)} \quad (119)$$

$$\begin{aligned}D(s)=\;&s^2C_1C_3\beta_{b1}+sC_3g_{mB1}^{(1)}\beta_{a1}\gamma_{b1}(-\beta_{b1}^2\\&+\beta_{a1}\beta_{b2}\beta_{b3}+\beta_{a1}\beta_{b3}^2-\beta_{a2}\beta_{b3}\beta_{b1}\\&+\beta_{a3}\beta_{b2}\gamma_{b1}A_1+\beta_{a3}\beta_{b3}\gamma_{b1}A_1)\\&+g_{mA1}^{(1)}g_{mB1}^{(1)}\beta_{a1}\beta_{b2}\gamma_{a1}\gamma_{b1}\end{aligned} \quad (120)$$

The pole frequency (ω_o), quality factor (Q_o) and bandwidth (BW) are:

$$\omega_o=\sqrt{\frac{g_{mA1}^{(1)}g_{mB1}^{(1)}\beta_{a1}\beta_{b2}\gamma_{a1}\gamma_{b1}}{C_1C_3\beta_{b1}}},$$

$$\begin{aligned}Q_o=\;&\frac{1}{(-\beta_{b1}^2+\beta_{a1}\beta_{b2}\beta_{b3}}\sqrt{\frac{C_1g_{mA1}^{(1)}\beta_{b2}\gamma_{a1}}{C_3g_{mB1}^{(1)}\beta_{a1}\beta_{b1}\gamma_{b1}}}\\&+\beta_{a1}\beta_{b3}^2-\beta_{a2}\beta_{b3}\beta_{b1}\\&+\beta_{a3}\beta_{b2}\gamma_{b1}A_1\\&+\beta_{a3}\beta_{b3}\gamma_{b1}A_1)\\&g_{mB1}^{(1)}\beta_{a1}\gamma_{b1}(-\beta_{b1}^2+\beta_{a1}\beta_{b2}\beta_{b3}\\&+\beta_{a1}\beta_{b3}^2-\beta_{a2}\beta_{b3}\beta_{b1}\end{aligned} \quad (121)$$

$$and\ BW=\frac{+\beta_{a3}\beta_{b2}\gamma_{b1}A_1+\beta_{a3}\beta_{b3}\gamma_{b1}A_1)}{C_1\beta_{b1}}$$

Current mode:

$$\frac{I_{LP}}{I_{in}}=\frac{g_{mB2}^{(1)}g_{mB3}^{(1)}\gamma_{b2}\gamma_{b3}}{D(s)} \quad (122)$$

$$\frac{I_{BP}}{I_{in}}=\frac{sC_2g_{mB2}^{(1)}\gamma_{b2}}{D(s)} \quad (123)$$

$$\frac{I_{HP}}{I_{in}}=-\frac{s^2C_1C_2}{D(s)} \quad (124)$$

$$\frac{I_{BR}}{I_{in}}=\frac{s^2C_1C_2+g_{mB2}^{(1)}g_{mB3}^{(1)}\gamma_{b2}\gamma_{b3}}{D(s)} \quad (125)$$

$$\frac{I_{AP}}{I_{in}}=\frac{\left(s^2C_1C_2-sC_2g_{mB2}^{(1)}\gamma_{b2}+g_{mB2}^{(1)}g_{mB3}^{(1)}\gamma_{b2}\gamma_{b3}\right)}{D(s)} \quad (126)$$

Where,

$$\begin{aligned}D(s)=\;&s^2C_1C_2+\left(1+A_2\gamma_{a1}\alpha_a\right)sC_2g_{mB2}^{(1)}\gamma_{b2}\\&+g_{mB2}^{(1)}g_{mB3}^{(1)}\gamma_{b2}\gamma_{b3}\end{aligned} \quad (127)$$

The pole frequency (ω_o), quality factor (Q_o) and bandwidth (BW) are:

$$\omega_o=\sqrt{\frac{g_{mB2}^{(1)}g_{mB3}^{(1)}\gamma_{b2}\gamma_{b3}}{C_1C_2}},$$

$$Q_o=\frac{1}{\left(1+A_2\gamma_{a1}\alpha_a\right)}\sqrt{\frac{C_1g_{mB3}^{(1)}\gamma_{b3}}{C_2g_{mB2}^{(1)}\gamma_{b2}}} \quad (128)$$

$$and\ BW=\left(1+A_2\gamma_{a1}\alpha_a\right)\frac{g_{mB2}^{(1)}\gamma_{b2}}{C_1}$$

The transfer function of Fig. 7 after considering the non-idealities are obtained as:

Voltage mode (VM):

$$\frac{V_{LP}}{V_{in}}=-\frac{g_{mA1}^{(1)}g_{mB1}^{(1)}\begin{pmatrix}\beta_{a1}\\-A_1\beta_{a3}\beta_{b1\gamma_{b1}}\end{pmatrix}\beta_{a1}\beta_{b2}\gamma_{a1}\gamma_{b1}}{D(s)} \quad (129)$$

$$\frac{V_{BP}}{V_{in}}=\frac{sC_3g_{mB1}^{(1)}\beta_{b2}\gamma_{B1}\left(\beta_{a1}-A_1\beta_{a3}\beta_{b1\gamma_{b1}}\right)}{D(s)} \quad (130)$$

$$\frac{V_{HP}}{V_{in}}=\frac{s^2C_1C_3\beta_{b2}\left(\beta_{a1}-A_1\beta_{a3}\beta_{b1\gamma_{b1}}\right)}{D(s)} \quad (131)$$

$$\frac{V_{AP}}{V_{in}}=-\frac{\begin{pmatrix}s^2C_1C_3\beta_{b2}-sC_3g_{mB1}^{(1)}\beta_{b2}\gamma_{B1}\\+g_{mA1}^{(1)}g_{mB1}^{(1)}\beta_{a1}\beta_{b2}\gamma_{a1}\gamma_{b1}\end{pmatrix}}{D(s)} \quad (132)$$

$$\frac{V_{BR}}{V_{in}}=\frac{\begin{pmatrix}s^2C_1C_3\beta_{b2}\\+g_{mA1}^{(1)}g_{mB1}^{(1)}\beta_{a1}\beta_{b2}\gamma_{a1}\gamma_{b1}\end{pmatrix}\begin{pmatrix}\beta_{a1}\\-A_1\beta_{a3}\beta_{b1\gamma_{b1}}\end{pmatrix}}{D(s)} \quad (133)$$

Transimpedance mode (TIM):

$$\frac{V_{LP}}{I_{in}} = -\frac{g_{mA1}^{(1)} g_{mB1}^{(1)} R_{in} \begin{pmatrix} \beta_{a1} \\ -A_1 \beta_{a3} \beta_{b1\gamma_{b1}} \end{pmatrix} \beta_{a1} \beta_{b2} \gamma_{a1} \gamma_{b1}}{D(s)} \quad (134)$$

$$\frac{V_{BP}}{I_{in}} = \frac{sC_3 g_{mB1}^{(1)} R_{in} \beta_{b2} \gamma_{B1} \left(\beta_{a1} - A_1 \beta_{a3} \beta_{b1\gamma_{b1}} \right)}{D(s)} \quad (135)$$

$$\frac{V_{HP}}{I_{in}} = \frac{s^2 C_1 C_3 R_{in} \beta_{b2} \left(\beta_{a1} - A_1 \beta_{a3} \beta_{b1\gamma_{b1}} \right)}{D(s)} \quad (136)$$

$$\frac{V_{AP}}{I_{in}} = -\frac{\begin{pmatrix} s^2 C_1 C_3 \beta_{b2} - sC_3 g_{mB1}^{(1)} \beta_{b2} \gamma_{B1} \\ + g_{mA1}^{(1)} g_{mB1}^{(1)} \beta_{a1} \beta_{b2} \gamma_{a1} \gamma_{b1} \end{pmatrix} R_{in}}{D(s)} \quad (137)$$

$$\frac{V_{BR}}{I_{in}} = \frac{\begin{pmatrix} s^2 C_1 C_3 \beta_{b2} \\ + g_{mA1}^{(1)} g_{mB1}^{(1)} \beta_{a1} \beta_{b2} \gamma_{a1} \gamma_{b1} \end{pmatrix} \begin{pmatrix} \beta_{a1} \\ -A_1 \beta_{a3} \beta_{b1\gamma_{b1}} \end{pmatrix} R_{in}}{D(s)} \quad (138)$$

Where,

$$D(s) = s^2 C_1 C_3 + sC_3 g_{mB1}^{(1)} \beta_{a1} \gamma_{b1} \begin{pmatrix} 1 + \beta_{a2} \\ -\beta_{a3} \beta_{b2} \gamma_{b1} A_1 - \beta_{a3} \beta_{b3} \gamma_{b1} A_1 \end{pmatrix} + g_{mA1}^{(1)} g_{mB1}^{(1)} \beta_{a1} \beta_{b2} \gamma_{a1} \gamma_{b1} \quad (139)$$

The pole frequency (ω_o), quality factor (Q_o) and bandwidth (BW) are:

$$\omega_o = \sqrt{\frac{g_{mA1}^{(1)} g_{mB1}^{(1)} \beta_{a1} \beta_{b2} \gamma_{a1} \gamma_{b1}}{C_1 C_3}},$$

$$Q_o = \frac{1}{\begin{matrix} 1 + \beta_{a2} \\ -\beta_{a3} \beta_{b2} \gamma_{b1} A_1 - \beta_{a3} \beta_{b3} \gamma_{b1} A_1 \end{matrix}} \sqrt{\frac{C_1 g_{mA1}^{(1)} \beta_{b2} \gamma_{a1}}{C_3 g_{mB1}^{(1)} \beta_{a1} \beta_{b1} \gamma_{b1}}} \quad (140)$$

$$BW = \beta_{a1} \gamma_{b1} \begin{pmatrix} 1 + \beta_{a2} \\ -\beta_{a3} \beta_{b2} \gamma_{b1} A_1 - \beta_{a3} \beta_{b3} \gamma_{b1} A_1 \end{pmatrix} \frac{g_{mB1}^{(1)}}{C_1}$$

Current mode (CM):

$$\frac{I_{LP}}{I_{in}} = \frac{g_{mB2}^{(1)} g_{mB3}^{(1)} \gamma_{b2} \gamma_{b3}}{D(s)} \quad (141)$$

$$\frac{I_{BP}}{I_{in}} = \frac{sC_2 g_{mB2}^{(1)} \gamma_{b2}}{D(s)} \quad (142)$$

$$\frac{I_{HP}}{I_{in}} = \frac{s^2 C_1 C_2}{D(s)} \quad (143)$$

$$\frac{I_{BR}}{I_{in}} = \frac{s^2 C_1 C_2 + g_{mB2}^{(1)} g_{mB3}^{(1)} \gamma_{b2} \gamma_{b3}}{D(s)} \quad (144)$$

$$\frac{I_{AP}}{I_{in}} = \frac{\left(s^2 C_1 C_2 - sC_2 g_{mB2}^{(1)} \gamma_{b2} + g_{mB2}^{(1)} g_{mB3}^{(1)} \gamma_{b2} \gamma_{b3} \right)}{D(s)} \quad (145)$$

Transadmittance mode (TAM) [with $I_{in1} = 0$]:

$$\frac{I_{LP}}{V_{in}} = \frac{g_{mB2}^{(1)} g_{mB3}^{(1)} \gamma_{b2} \gamma_{b3}}{D(s) * R_{in}} \quad (146)$$

$$\frac{I_{BP}}{V_{in}} = \frac{sC_2 g_{mB2}^{(1)} \gamma_{b2}}{D(s) * R_{in}} \quad (147)$$

$$\frac{I_{HP}}{V_{in}} = \frac{s^2 C_1 C_2}{D(s) * R_{in}} \quad (148)$$

$$\frac{I_{BR}}{V_{in}} = \frac{s^2 C_1 C_2 + g_{mB2}^{(1)} g_{mB3}^{(1)} \gamma_{b2} \gamma_{b3}}{D(s) * R_{in}} \quad (149)$$

$$\frac{I_{AP}}{V_{in}} = \frac{\left(s^2 C_1 C_2 - sC_2 g_{mB2}^{(1)} \gamma_{b2} + g_{mB2}^{(1)} g_{mB3}^{(1)} \gamma_{b2} \gamma_{b3} \right)}{D(s) * R_{in}} \quad (150)$$

Where,

$$D(s) = s^2 C_1 C_2 + \left(1 + A_2 \gamma_{a1} \alpha_a \right) sC_2 g_{mB2}^{(1)} \gamma_{b2} + g_{mB2}^{(1)} g_{mB3}^{(1)} \gamma_{b2} \gamma_{b3} \quad (151)$$

The pole frequency (ω_o), quality factor (Q_o) and bandwidth (BW) are:

$$\omega_o = \sqrt{\frac{g_{mB2}^{(1)} g_{mB3}^{(1)} \gamma_{b2} \gamma_{b3}}{C_1 C_2}},$$

$$Q_o = \frac{1}{\left(1 + A_2 \gamma_{a1} \alpha_a \right)} \sqrt{\frac{C_1 g_{mB3}^{(1)} \gamma_{b3}}{C_2 g_{mB2}^{(1)} \gamma_{b2}}} \quad (152)$$

$$and\ BW = \left(1 + A_2 \gamma_{a1} \alpha_a \right) \frac{g_{mB2}^{(1)} \gamma_{b2}}{C_1}$$

The effects caused due to non-idealities can be easily observed from the above eqns. (102, 114, 121, 128, 140, 152). However, if transfer gains are close to unity, which is normally the case, then these equations may revert into the ideal forms.

4.2 Effects of parasitics

The non-ideal equivalent circuit of FD-CCCTA is shown in Fig. 8. Series resistance at X_A and X_B terminals are of low value. $(C_{Y1} \| R_{Y1})$, $(C_{Y2} \| R_{Y2})$, $(C_{Y3} \| R_{Y3})$,

$(C_{Y4} \| R_{Y4})$, are at Y_1, Y_2, Y_3, and Y_4 terminals, respectively while $(C_{ZA} || R_{ZA})$, $(C_{ZB} \| R_{ZB})$, $(C_{OA1} \| R_{OA1})$, $(C_{OB1} \| R_{OB1})$, are at Z_A, Z_B, O_{A1}, and O_{B1} terminals. The values of R_{Y1}, R_{Y2}, R_{Y3}, R_{Y4}, R_{ZA}, R_{ZB}, R_{OA1}, R_{OB1} are high whereas C_{Y1}, C_{Y2}, C_{Y3}, C_{Y4}, C_{ZA}, C_{ZB}, C_{OA1}, C_{OB1} are low.

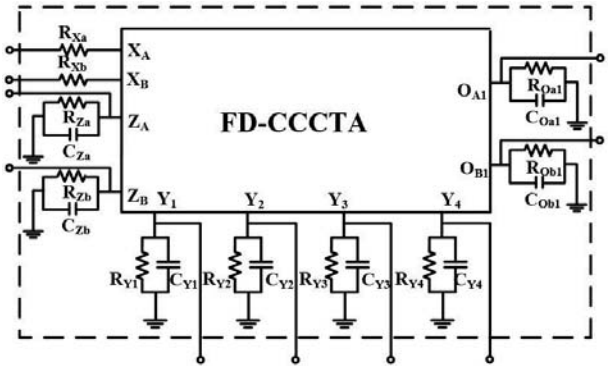

Figure 8: Non-ideal equivalent circuit of FD-CCCTA.

The non-ideal circuit of proposed mixed-mode filter is shown in Fig. 9 where impedances are:

$$Z_1 = \left(C_1' \left\| R_{Y1}^{(1)} \right\| R_{OB1}^{(1)}\right),\ Z_2 = (C_2' \| R_{OB2}^{(1)})$$

$$Z_3 = \left(C_3' \left\| R_{Y4}^{(1)} \right\| R_{OA1}^{(1)}\right),\ Z_4 = (C_{ZB}^{(1)} \| R_{ZB}^{(1)}),$$

$$Z_5 = (C_{ZA}^{(1)} \| R_{ZA}^{(1)})$$

$$Z_{in} = \left(C_{Y2}^{(1)} \left\| C_{Y3}^{(1)} \right\| R_{Y2}^{(1)} \left\| R_{Y3}^{(1)} \right\| R_{in}\right)$$

Where,

$$C_1' = C_1 + C_{OB1}^{(1)} + C_{Y1}^{(1)},\ C_2' = C_2 + C_{OB2}^{(1)},$$

$$C_3' = C_3 + C_{OA1}^{(1)} + C_{Y4}^{(1)}$$

The routine analysis of Fig. 9 results in:

Voltage Mode (VM):

$$\frac{V_{LP}}{V_{in}} = -\frac{g_{mA1}^{(1)} g_{mB1}^{(1)}}{D(s)} \tag{153}$$

$$\frac{V_{BP}}{V_{in}} = \frac{\left(sC_3' + \frac{1}{R_{Y4}} + \frac{1}{R_{OA1}}\right) g_{mB1}^{(1)}}{D(s)} \tag{154}$$

$$\frac{V_{HP}}{V_{in}} = \frac{\left(sC_1' + \frac{1}{R_{Y1}} + \frac{1}{R_{OB1}}\right)\left(sC_3' + \frac{1}{R_{Y4}} + \frac{1}{R_{OA1}}\right)}{D(s)} \tag{155}$$

$$\frac{V_{BR}}{V_{in}} = -\frac{\left(\left(sC_1' + \frac{1}{R_{Y1}} + \frac{1}{R_{OB1}}\right)\left(sC_3' + \frac{1}{R_{Y4}} + \frac{1}{R_{OA1}}\right) + g_{mA1}^{(1)} g_{mB1}^{(1)}\right)}{D(s)} \tag{156}$$

$$\frac{V_{AP}}{V_{in}} = -\frac{\left(\begin{array}{l}\left(sC_1' + \frac{1}{R_{Y1}} + \frac{1}{R_{OB1}}\right)\\ \left(sC_3' + \frac{1}{R_{Y4}} + \frac{1}{R_{OA1}}\right) -\\ \left(sC_3' + \frac{1}{R_{Y4}} + \frac{1}{R_{OA1}}\right) g_{mB1}^{(1)}\\ + g_{mA1}^{(1)} g_{mB1}^{(1)}\end{array}\right)}{D(s)} \tag{157}$$

Transimpedance Mode (TIM):

$$\frac{V_{LP}}{I_{in}} = -\frac{g_{mA1}^{(1)} g_{mB1}^{(1)} R_{in}}{D(s)} \tag{158}$$

$$\frac{V_{BP}}{I_{in}} = \frac{\left(sC_3' + \frac{1}{R_{Y4}} + \frac{1}{R_{OA1}}\right) g_{mB1}^{(1)} R_{in}}{D(s)} \tag{159}$$

$$\frac{V_{HP}}{I_{in}} = \frac{\left(sC_1' + \frac{1}{R_{Y1}} + \frac{1}{R_{OB1}}\right)\left(sC_3' + \frac{1}{R_{Y4}} + \frac{1}{R_{OA1}}\right) R_{in}}{D(s)} \tag{160}$$

$$\frac{V_{BR}}{I_{in}} = -\frac{\left(\left(sC_1' + \frac{1}{R_{Y1}} + \frac{1}{R_{OB1}}\right)\left(sC_3' + \frac{1}{R_{Y4}} + \frac{1}{R_{OA1}}\right) + g_{mA1}^{(1)} g_{mB1}^{(1)}\right) R_{in}}{D(s)} \tag{161}$$

$$\frac{V_{AP}}{I_{in}} = -\frac{\left(\begin{array}{l}\left(sC_1' + \frac{1}{R_{Y1}} + \frac{1}{R_{OB1}}\right)\\ \left(sC_3' + \frac{1}{R_{Y4}} + \frac{1}{R_{OA1}}\right) -\\ \left(sC_3' + \frac{1}{R_{Y4}} + \frac{1}{R_{OA1}}\right) g_{mB1}^{(1)}\\ + g_{mA1}^{(1)} g_{mB1}^{(1)}\end{array}\right) R_{in}}{D(s)} \tag{162}$$

Where,

$$D(s)=\left(sC_1'+\frac{1}{R_{Y1}}+\frac{1}{R_{OB1}}\right)\left(sC_3'+\frac{1}{R_{Y4}}+\frac{1}{R_{OA1}}\right)+\left(sC_3'+\frac{1}{R_{Y4}}+\frac{1}{R_{OA1}}\right)g_{mB1}^{(1)}+g_{mA1}^{(1)}g_{mB1}^{(1)} \quad (163)$$

Current Mode (CM):

$$\frac{I_{LP}}{I_{in}}=\frac{g_{mB2}^{(1)}g_{mB3}^{(1)}}{D(s)} \quad (164)$$

$$\frac{I_{BP}}{I_{in}}=\frac{\left(sC_2'+\frac{1}{R_{OB2}}\right)g_{mB2}^{(1)}}{D(s)} \quad (165)$$

$$\frac{I_{HP}}{I_{in}}=\frac{\left(sC_1'+\frac{1}{R_{Y1}}+\frac{1}{R_{OB1}}\right)\left(sC_2'+\frac{1}{R_{OB2}}\right)}{D(s)} \quad (166)$$

$$\frac{I_{BR}}{I_{in}}=\frac{\left(sC_1'+\frac{1}{R_{Y1}}+\frac{1}{R_{OB1}}\right)\left(sC_2'+\frac{1}{R_{OB2}}\right)+g_{mB2}^{(1)}g_{mB3}^{(1)}}{D(s)} \quad (167)$$

$$\frac{I_{AP}}{I_{in}}=\frac{\left(sC_1'+\frac{1}{R_{Y1}}+\frac{1}{R_{OB1}}\right)\left(sC_2'+\frac{1}{R_{OB2}}\right)-\left(sC_2'+\frac{1}{R_{OB2}}\right)g_{mB2}^{(1)}+g_{mB2}^{(1)}g_{mB3}^{(1)}}{D(s)} \quad (168)$$

Transadmittance Mode (TAM):

$$\frac{I_{LP}}{V_{in}}=\frac{g_{mB2}^{(1)}g_{mB3}^{(1)}}{D(s)*R_{in}} \quad (169)$$

$$\frac{I_{BP}}{V_{in}}=\frac{\left(sC_2'+\frac{1}{R_{OB2}}\right)g_{mB2}^{(1)}}{D(s)*R_{in}} \quad (170)$$

$$\frac{I_{HP}}{V_{in}}=\frac{\left(sC_1'+\frac{1}{R_{Y1}}+\frac{1}{R_{OB1}}\right)\left(sC_2'+\frac{1}{R_{OB2}}\right)}{D(s)*R_{in}} \quad (171)$$

$$\frac{I_{BR}}{V_{in}}=\frac{\left(sC_1'+\frac{1}{R_{Y1}}+\frac{1}{R_{OB1}}\right)\left(sC_2'+\frac{1}{R_{OB2}}\right)+g_{mB2}^{(1)}g_{mB3}^{(1)}}{D(s)*R_{in}} \quad (172)$$

$$\frac{I_{AP}}{V_{in}}=\frac{\left(sC_1'+\frac{1}{R_{Y1}}+\frac{1}{R_{OB1}}\right)\left(sC_2'+\frac{1}{R_{OB2}}\right)-\left(sC_2'+\frac{1}{R_{OB2}}\right)g_{mB2}^{(1)}+g_{mB2}^{(1)}g_{mB3}^{(1)}}{D(s)*R_{in}} \quad (173)$$

Where,

$$D(s)=\left(sC_1'+\frac{1}{R_{Y1}}+\frac{1}{R_{OB1}}\right)\left(sC_2'+\frac{1}{R_{OB2}}\right)+\left(sC_2'+\frac{1}{R_{OB2}}\right)g_{mB2}^{(1)}+g_{mB2}^{(1)}g_{mB3}^{(1)} \quad (174)$$

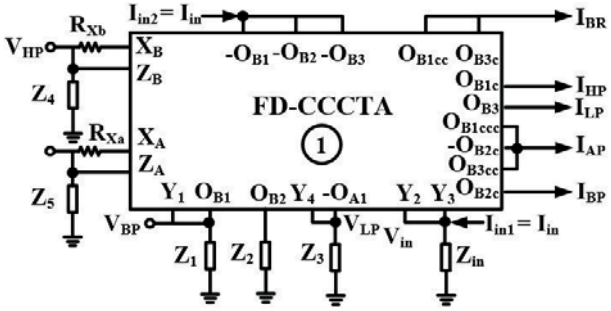

Figure 9: Non-ideal equivalent circuit of Fig. 3 with parasitics.

The non-ideal circuit of proposed mixed-mode first shadow filter (Fig. 6) is shown in Fig. 10, where impedances are:

$$Z_6=\left(C_{Y2}^{(1)}\left\|C_{Y3}^{(1)}\right.\|\left.R_{Y2}^{(1)}\right\|R_{Y3}^{(1)}\right),$$

$$Z_7=\left(C_{Y1}^{(2)}\left\|C_{ZB}^{(2)}\right.\|\left.R_{Y1}^{(2)}\right\|R_{ZB}^{(2)}\right),$$

$$Z_8=\left(C_{Y3}^{(2)}\left\|C_{OB}^{(2)}\right.\|\left.R_{Y3}^{(2)}\right\|R_{OB}^{(2)}\|R_1\right),$$

$$Z_9=(C_{ZA}^{(2)}\left|\right.R_{ZA}^{(2)}\left|\right.|R_2),$$

The rest of the impedances are similar to the Fig. 8 The routine analysis of Fig. 10 results VM, and CM expressions due to the effect of parasitics as:

Voltage mode:

$$\frac{V_{LP}}{V_{in}}=\frac{g_{mA1}^{(1)}g_{mB1}^{(1)}\left(1+A_1\right)}{D(s)} \quad (175)$$

$$\frac{V_{BP}}{V_{in}}=\frac{\left(sC_3'+\frac{1}{R_{Y4}}+\frac{1}{R_{OA1}}\right)g_{mB1}^{(1)}\left(1+A_1\right)}{D(s)} \quad (176)$$

$$\left(sC_1'+\frac{1}{R_{Y1}}+\frac{1}{R_{OB1}}\right)$$

$$\frac{V_{HP}}{V_{in}}=-\frac{\left(sC_3'+\frac{1}{R_{Y4}}+\frac{1}{R_{OA1}}\right)\left(1+A_1\right)}{D(s)} \quad (178)$$

$$\frac{V_{AP}}{V_{in}}=-\frac{\left(\begin{array}{c}\left(sC_1'+\frac{1}{R_{Y1}}+\frac{1}{R_{OB1}}\right)\\ \left(sC_3'+\frac{1}{R_{Y4}}+\frac{1}{R_{OA1}}\right)-\\ \left(sC_3'+\frac{1}{R_{Y4}}+\frac{1}{R_{OA1}}\right)g_{mB1}^{(1)}\\ +g_{mA1}^{(1)}g_{mB1}^{(1)}\end{array}\right)}{D(s)} \quad (179)$$

$$\frac{V_{BR}}{V_{in}}=\frac{\left(\begin{array}{c}\left(sC_1'+\frac{1}{R_{Y1}}+\frac{1}{R_{OB1}}\right)\\ \left(sC_3'+\frac{1}{R_{Y4}}+\frac{1}{R_{OA1}}\right)\left(1+A_1\right)\\ +g_{mA1}^{(1)}g_{mB1}^{(1)}\end{array}\right)}{D(s)} \quad (180)$$

Where,

$$A_1=g_{mB}^{(2)}Z_8$$

$$D(s)=\left(sC_1'+\frac{1}{R_{Y1}}+\frac{1}{R_{OB1}}\right)\left(sC_3'+\frac{1}{R_{Y4}}+\frac{1}{R_{OA1}}\right)+2A_1\left(sC_3'+\frac{1}{R_{Y4}}+\frac{1}{R_{OA1}}\right)g_{mB1}^{(1)}+g_{mA1}^{(1)}g_{mB1}^{(1)}-I_{XA}^{(2)}Z_6 \quad (181)$$

Current mode:

$$\frac{I_{LP}}{I_{in}}=\frac{g_{mB2}^{(1)}g_{mB3}^{(1)}}{D(s)} \quad (182)$$

$$\frac{I_{BP}}{I_{in}}=\frac{\left(sC_2'+\frac{1}{R_{OB2}}\right)g_{mB2}^{(1)}}{D(s)} \quad (183)$$

$$\frac{I_{HP}}{I_{in}}=-\frac{\left(sC_1'+\frac{1}{R_{Y1}}+\frac{1}{R_{OB1}}\right)\left(sC_2'+\frac{1}{R_{OB2}}\right)}{D(s)} \quad (184)$$

$$\left(sC_1'+\frac{1}{R_{Y1}}+\frac{1}{R_{OB1}}\right)\left(sC_2'+\frac{1}{R_{OB2}}\right)$$

$$\frac{I_{BR}}{I_{in}}=\frac{+g_{mB2}^{(1)}g_{mB3}^{(1)}}{D(s)} \quad (185)$$

$$\left(sC_1'+\frac{1}{R_{Y1}}+\frac{1}{R_{OB1}}\right)\left(sC_2'+\frac{1}{R_{OB2}}\right)$$

$$\frac{I_{AP}}{I_{in}}=\frac{-\left(sC_2'+\frac{1}{R_{OB2}}\right)g_{mB2}^{(1)}+g_{mB2}^{(1)}g_{mB3}^{(1)}}{D(s)} \quad (186)$$

Where,

$$D(s)=\left(sC_1'+\frac{1}{R_{Y1}}+\frac{1}{R_{OB1}}\right)\left(sC_2'+\frac{1}{R_{OB2}}\right)+\left(1+A_2\right)\left(sC_2'+\frac{1}{R_{OB2}}\right)g_{mB2}^{(1)}+g_{mB2}^{(1)}g_{mB3}^{(1)} \quad (187)$$

$$and\ A_2=g_{mA}^{(2)}Z_9$$

Similarly, the non-ideal circuit of proposed mixed-mode second shadow filter (Fig. 7) is shown in Fig. 11, where impedances are:

$$Z_7=\left(C_{Y1}^{(2)}\parallel R_{Y1}^{(2)}\parallel R_{in}\right),\ Z_{10}=(C_{ZB}^{(2)}\parallel R_{ZB}^{(2)})$$

While rest of the impedances are similar to the Fig. 8 and Fig. 9. The routine analysis of Fig. 11 results VM, TIM, CM, and TAM expressions due to the effect of parasitics as follows:

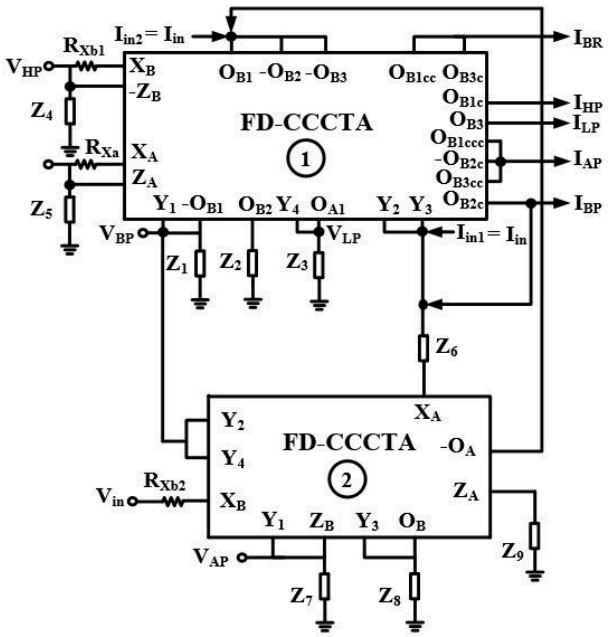

Figure 10: Non-ideal equivalent circuit of Fig. 6 with parasitics.

Voltage mode (VM):

$$\frac{V_{LP}}{V_{in}}=-\frac{g_{mA1}^{(1)}g_{mB1}^{(1)}\left(1-A_1\right)}{D(s)} \quad (188)$$

$$\frac{V_{BP}}{V_{in}}=\frac{\left(sC_3'+\frac{1}{R_{Y4}}+\frac{1}{R_{OA1}}\right)g_{mB1}^{(1)}\left(1-A_1\right)}{D(s)} \quad (189)$$

$$\frac{V_{HP}}{V_{in}}=\frac{\left(sC_3'+\frac{1}{R_{Y4}}+\frac{1}{R_{OA1}}\right)\left(1-A_1\right)}{D(s)} \quad (190)$$

$$\frac{V_{BR}}{V_{in}}=\frac{\left(\begin{array}{c}\left(sC_1'+\frac{1}{R_{Y1}}+\frac{1}{R_{OB1}}\right)\\ \left(sC_3'+\frac{1}{R_{Y4}}+\frac{1}{R_{OA1}}\right)\\ +g_{mA1}^{(1)}g_{mB1}^{(1)}\end{array}\right)\left(1-A_1\right)}{D(s)} \quad (191)$$

$$\frac{V_{AP}}{V_{in}}=-\frac{\left(\begin{array}{c}\left(sC_1'+\frac{1}{R_{Y1}}+\frac{1}{R_{OB1}}\right)\\ \left(sC_3'+\frac{1}{R_{Y4}}+\frac{1}{R_{OA1}}\right)\\ -\left(sC_3'+\frac{1}{R_{Y4}}+\frac{1}{R_{OA1}}\right)g_{mB1}^{(1)}\\ +g_{mA1}^{(1)}g_{mB1}^{(1)}\end{array}\right)}{D(s)} \quad (192)$$

Transimpedance mode (TIM):

$$\frac{V_{LP}}{I_{in}}=-\frac{g_{mA1}^{(1)}g_{mB1}^{(1)}R_{in}\left(1-A_1\right)}{D(s)} \quad (193)$$

$$\frac{V_{BP}}{I_{in}}=\frac{\left(sC_3'+\frac{1}{R_{Y4}}+\frac{1}{R_{OA1}}\right)g_{mB1}^{(1)}R_{in}\left(1-A_1\right)}{D(s)} \quad (194)$$

$$\frac{V_{HP}}{I_{in}}=\frac{\left(sC_1'+\frac{1}{R_{Y1}}+\frac{1}{R_{OB1}}\right)\left(sC_3'+\frac{1}{R_{Y4}}+\frac{1}{R_{OA1}}\right)\left(1-A_1\right)R_{in}}{D(s)} \quad (195)$$

$$\frac{V_{BR}}{I_{in}}=\frac{\left(\begin{array}{c}\left(sC_1'+\frac{1}{R_{Y1}}+\frac{1}{R_{OB1}}\right)\\ \left(sC_3'+\frac{1}{R_{Y4}}+\frac{1}{R_{OA1}}\right)\\ +g_{mA1}^{(1)}g_{mB1}^{(1)}\end{array}\right)R_{in}\left(1-A_1\right)}{D(s)} \quad (196)$$

$$\frac{V_{AP}}{I_{in}}=-\frac{\left(\begin{array}{c}\left(sC_1'+\frac{1}{R_{Y1}}+\frac{1}{R_{OB1}}\right)\\ \left(sC_3'+\frac{1}{R_{Y4}}+\frac{1}{R_{OA1}}\right)-\\ \left(sC_3'+\frac{1}{R_{Y4}}+\frac{1}{R_{OA1}}\right)g_{mB1}^{(1)}\\ +g_{mA1}^{(1)}g_{mB1}^{(1)}\end{array}\right)R_{in}}{D(s)} \quad (197)$$

Where,

$$A_1 = g_{mB}^{(2)} Z_8$$

$$D(s) = \left(sC_1' + \frac{1}{R_{Y1}} + \frac{1}{R_{OB1}} \right)\left(sC_3' + \frac{1}{R_{Y4}} + \frac{1}{R_{OA1}} \right) + 2(1 - A_1)\left(sC_3' + \frac{1}{R_{Y4}} + \frac{1}{R_{OA1}} \right) g_{mB1}^{(1)} + g_{mA1}^{(1)} g_{mB1}^{(1)} - I_{XA}^{(2)} Z_6 \quad (198)$$

Current mode (CM):

$$\frac{I_{LP}}{I_{in}} = \frac{g_{mB2}^{(1)} g_{mB3}^{(1)}}{D(s)} \quad (199)$$

$$\frac{I_{BP}}{I_{in}} = \frac{\left(sC_2' + \frac{1}{R_{OB2}} \right) g_{mB2}^{(1)}}{D(s)} \quad (200)$$

$$\frac{I_{HP}}{I_{in}} = \frac{\left(sC_1' + \frac{1}{R_{Y1}} + \frac{1}{R_{OB1}} \right)\left(sC_2' + \frac{1}{R_{OB2}} \right)}{D(s)} \quad (201)$$

$$\frac{I_{BR}}{I_{in}} = \frac{\left(sC_1' + \frac{1}{R_{Y1}} + \frac{1}{R_{OB1}} \right)\left(sC_2' + \frac{1}{R_{OB2}} \right) + g_{mB2}^{(1)} g_{mB3}^{(1)}}{D(s)} \quad (202)$$

$$\frac{I_{AP}}{I_{in}} = \frac{\left(sC_1' + \frac{1}{R_{Y1}} + \frac{1}{R_{OB1}} \right)\left(sC_2' + \frac{1}{R_{OB2}} \right) - \left(sC_2' + \frac{1}{R_{OB2}} \right) g_{mB2}^{(1)} + g_{mB2}^{(1)} g_{mB3}^{(1)}}{D(s)} \quad (203)$$

Transadmittance mode (TAM):

$$\frac{I_{LP}}{V_{in}} = \frac{g_{mB2}^{(1)} g_{mB3}^{(1)}}{D(s) * R_{in}} \quad (204)$$

$$\frac{I_{BP}}{V_{in}} = \frac{\left(sC_2' + \frac{1}{R_{OB2}} \right) g_{mB2}^{(1)}}{D(s) * R_{in}} \quad (205)$$

$$\frac{I_{HP}}{V_{in}} = \frac{\left(sC_1' + \frac{1}{R_{Y1}} + \frac{1}{R_{OB1}} \right)\left(sC_2' + \frac{1}{R_{OB2}} \right)}{D(s) * R_{in}} \quad (206)$$

$$\frac{I_{BR}}{V_{in}} = \frac{\left(sC_1' + \frac{1}{R_{Y1}} + \frac{1}{R_{OB1}} \right)\left(sC_2' + \frac{1}{R_{OB2}} \right) + g_{mB2}^{(1)} g_{mB3}^{(1)}}{D(s) * R_{in}} \quad (207)$$

$$\frac{I_{AP}}{V_{in}} = \frac{\left(sC_1' + \frac{1}{R_{Y1}} + \frac{1}{R_{OB1}} \right)\left(sC_2' + \frac{1}{R_{OB2}} \right) - \left(sC_2' + \frac{1}{R_{OB2}} \right) g_{mB2}^{(1)} + g_{mB2}^{(1)} g_{mB3}^{(1)}}{D(s) * R_{in}} \quad (208)$$

Where,

$$D(s) = \left(sC_1' + \frac{1}{R_{Y1}} + \frac{1}{R_{OB1}} \right)\left(sC_2' + \frac{1}{R_{OB2}} \right) + (1 + A_2)\left(sC_2' + \frac{1}{R_{OB2}} \right) g_{mB2}^{(1)} + g_{mB2}^{(1)} g_{mB3}^{(1)} \quad (209)$$

$$and\ A_2 = g_{mA}^{(2)} Z_9$$

The above eqns. (153-209) show the effect of parasitics in the proposed mixed-mode filter, mixed-mode first shadow filter, and mixed-mode second shadow filter. However, the effect of parasitic capacitance can be neglected by suitably choosing the value of C_1, C_2, and

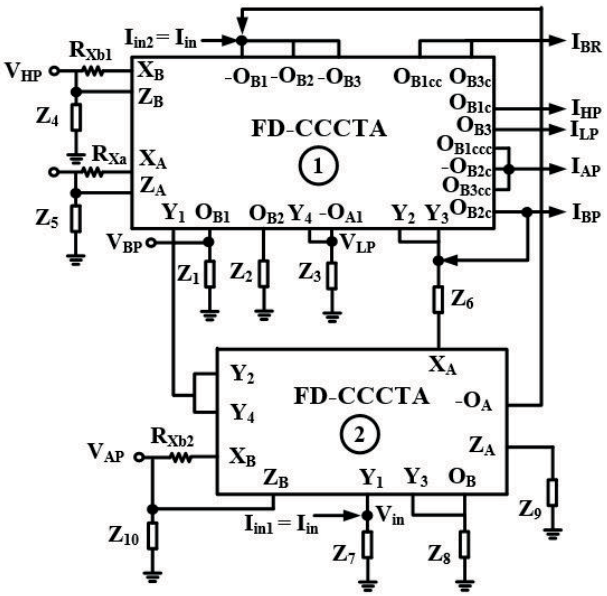

Figure 11: Non-ideal equivalent circuit of Fig. 7 with parasitics.

C_3 . While parasitic resistances, except R_X, can be easily neglected as it is high valued in the order of few MΩ.

5 Comparative analysis

The non-shadow mixed-mode universal filter is compared to state of the art in section 5.1, followed by section 5.2, wherein mixed-mode shadow filters are compared.

5.1 Comparison with the existing SIMO mixed-mode non-shadow universal filters

Table 3 compares the proposed filter with the existing SIMO mixed-mode biquad non-shadow universal filters. All the topologies use more than one active building block except [11] and the proposed one. Moreover, more passive components are used in [3, 7, 10, 11] than in the proposed one. Further, one or more passive components are floating in [3, 6, 7, 10, 11]. The filters [3, 7, 8] require matching components to realize the responses. Additional circuitry is required to obtain the simultaneous responses for the VM in [4, 5, 8, 10, 12], TAM in [3, 5-8, 11], CM in [3-7, 11, 12], and TIM in [4, 5, 12]. Independent tuning of ω_o and Q_o is not possible in [5, 6, 9, 10], and electronic tuning is not possible in [3, 7, 8, 10, 11]. The topologies [3, 6, 9] consume less power than this work. However most of the filters are found to be partially cascadable including the proposed ones, only ref. [8] is fully cascadable.

5.2 Comparison with the existing different modes of shadow filters

Table 4 compares the proposed mixed-mode shadow filters with the existing literature. It is noted that there is no report of any mixed-mode shadow filters realization using the same topology in literature except the proposed one. The topologies [13-20] realize only VM responses. Similarly, topologies [21-28] realize only CM responses, and [29] realizes only TIM and TAM responses. Whereas the proposed mixed-mode shadow filter realizes all the mixed-mode filters without alteration of the topology. The comparison Table 4 is self-explanatory for other parameters and features.

6 Simulated results and discussions

The functionality of the proposed non-shadow and shadow mixed-mode filters is verified through the Cadence virtuoso spectre circuit simulator using TSMC

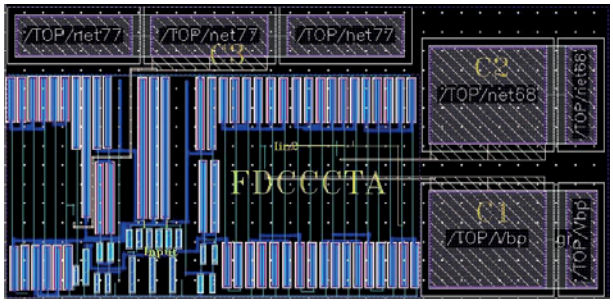

Figure 12: The layout of the proposed mixed-mode universal filter (Fig. 3).

180 nm technology. The DC biasing levels of FD-CCCTA are taken as $V_{DD} = 1.2$ V, $V_{SS} = -1.2$V, $V_{bp} = V_{bn} = 0$, $I_{bias1} = 25$ µA, $I_{bias2} = 20$ µA, and $I_{B1} = I_{A1} = 50$ µA. Table 1 gives the aspect ratios of the transistors. The non-shadow filter of Fig. 3 is implemented with passive components chosen as $C_1 = C_2 = C_3 = 1$ pF, and $R_{in} = 1$ Ω. Fig. 12 shows the layout of the mixed-mode universal filter of Fig. 3, which occupies an area of 158.5 µm x 76.3 µm. For the VM and TIM, the pre-layout and post-layout gain responses of LP, HP, BP, and BR are shown in Fig. 13 (a), and the gain and the phase responses of AP are shown in Fig. 13 (b). Similarly, the responses for CM and TAM are shown in Fig. 14. The calculated pole frequency and the qual-

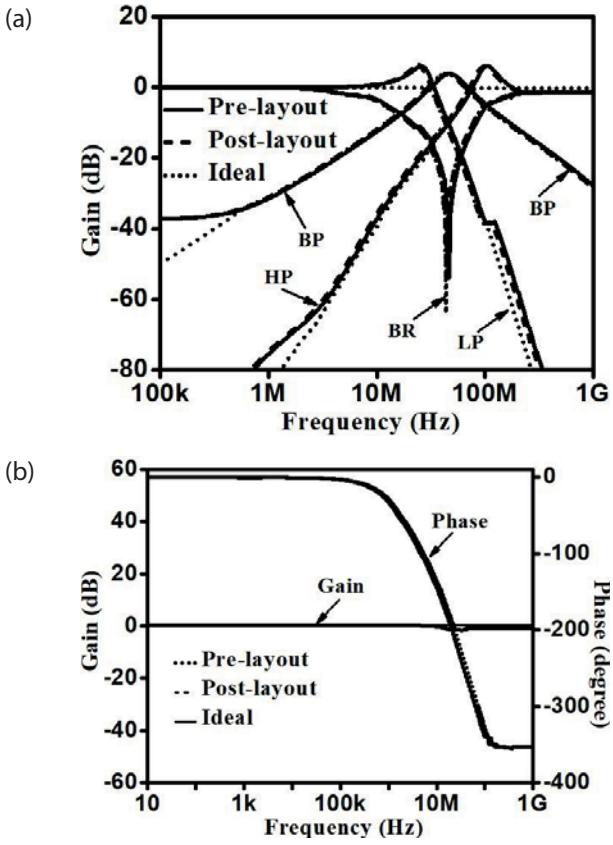

Figure 13: Simulated results of VM and TIM (Fig. 7) (a) gain responses of the LP, HP, BP, and BR (b) gain and phase responses of the AP filter.

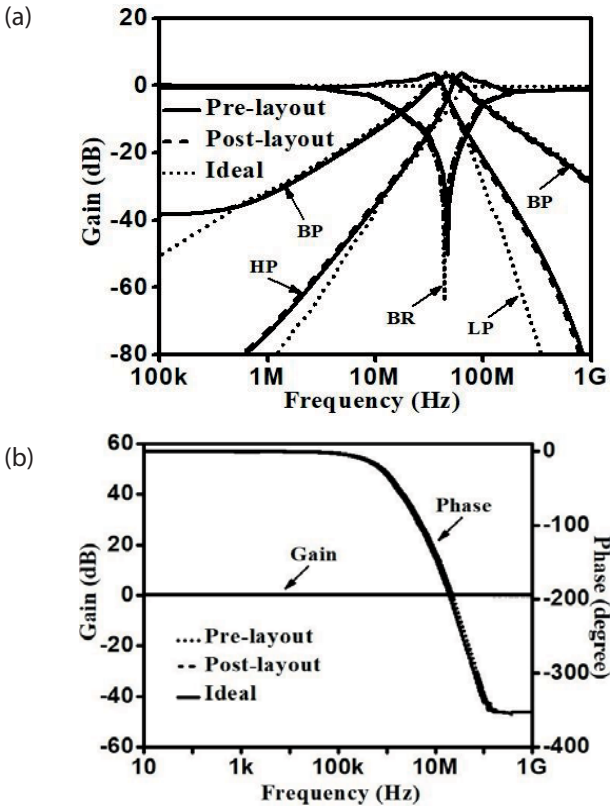

Figure 14: Simulated results of shadow CM and TAM (Fig. 7) (a) gain responses of the LP, HP, BP, BR (b) gain, and phase response of the AP filter.

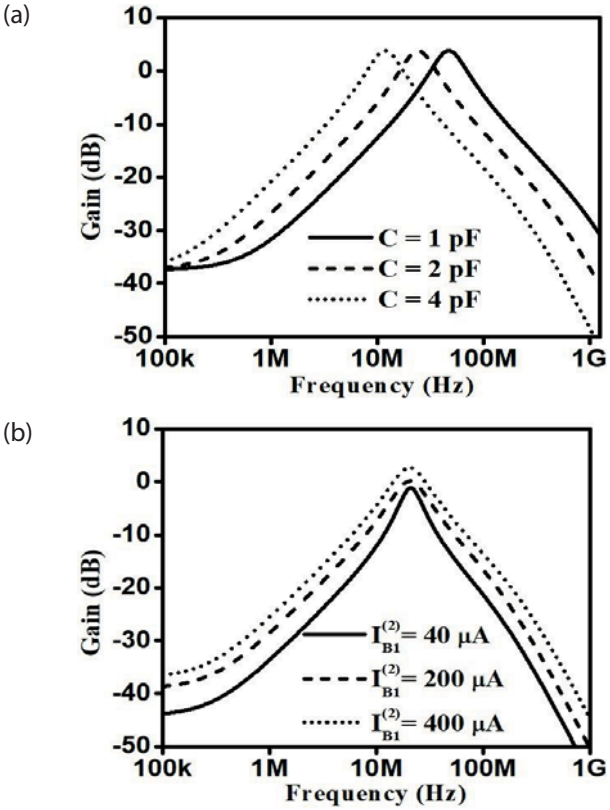

Figure 15: Simulated results of the VM shadow filter (Fig. 6) (a) tuning of fo due to capacitor value C, (b) tunability of Q, and gain due to A_1.

Table 3: Comparative analysis with the existing SIMO mixed-mode universal filters.

Ref.	No. & type of active elements used	No. of passive elements (R/C), All grounded elements (Yes/No)	Matching comp. req.	Simultaneous responses obtained {Input Imp./ Output Imp.}				Independent tuning of ω_o & Q_o	Electronic tuning	Power Cons. (mW)	Fully Cascadable
				VM	TAM	CM	TIM				
3.	2, FDCCII	4/2, No	Yes	UF {H/H}	LP, BP, HP {H/H}	LP, BP, HP, BR {H/H}	UF {H/H}	Yes	No	1.32	No
4.	3, CCCCTA	0/2, Yes	No	LP, BP, HP, BR {H/H}	UF {H/H}	LP, BP, HP {L/H}	LP, BP, HP {L/H}	Yes	Yes	1.99	No
5.	4, OTA	0/2, Yes	No	LP, BP, HP {H/H}	LP, BP, HP {H/H}	LP, BP, HP {H/H}	LP, BP, HP {H/H}	No	Yes	NA	No
6.	6, OTA	1/2, No	No	UF {L/H}	BP, HP {L/H}	BP, HP, BR {H/H}	UF {H/H}	No	Yes	1.57	No
7.	3, DDCC	4/2, No	Yes	UF {H/H}	LP, BP, HP {H/H}	LP, BP, HP {H/H}	UF {H/H}	Yes	No	NA	No
8.	3, DVCC, 6 MOS	0/2, 6 MOSs, Yes	Yes	LP, BP, BR {H/L}	LP, BP, HP {H/H}	LP, BP, HP {L/H}	LP, BP {L/L}	Yes	No	NA	Yes
9.	3, OTA 3, Diff. OTA	0/2, Yes	No	UF {H/H}	UF {H/H}	UF {H/H}	UF {H/H}	No	Yes	0.075	No
10.	3, FTFN	3/2, No	No	LP, BP, HP {L/H}	LP, BP, HP {L/L}	LP, BP, HP {L/L}	LP, BP, HP {L/H}	No	No	NA	No
11.	1, FDCCII	3/2, No	No	UF {L/H}	BP, HP {L/H}	BP, HP, BR {H/H}	UF {H/H}	Yes	No	NA	No
12.	5, MCCCII	0/2, Yes	No	LP, BP, HP {L/H}	LP, BP, HP {H/L}	LP, BP, HP {H/H}	LP, BP, HP {H/H}	Yes	Yes	NA	No
This work	1, FDCCCTA (Fig. 3)	1/3, Yes	No	LP, BP, HP {H/H}	UF {H/H}	UF {H/H}	LP, BP, HP {H/H}	Yes	Yes	1.9	No

Table 4: Comparative analysis with the existing different modes of shadow filters.

Ref.	No. & type of active elements used	No. of passive elements (R/C), All grounded elements (Yes/No)	Simultaneous responses obtained {Input Imp./ Output Imp.}				Independent tuning of w_o & Q_o	Electronic tuning	Power Cons. (mW)	Fully Cascadable
			VM	TAM	CM	TIM				
13.	4, CFOA	7/2, No	HP {H/H}	------	------	------	No	No	NA	No
14.	5, CFOA	9/2, No	BP {H/L}	------	------	------	Yes	No	NA	Yes
*15.	6, CFOA	10/2, No	LP, BP, HP, BR {H/L}	------	------	------	Yes	No	NA	Yes
16.	3, OTRA	11/4, No	LP, BP {H/H}	------	------	------	No	No	NA	No
17.	3, VDDDA	1/2, Yes	UF {H/H}	------	------	------	Yes	Yes	NA	No
18.	4, DDCC	5/2, Yes	LP, BP, HP {H/H}	------	------	------	Yes	No	NA	No
*19.	2, OP-AMP	2/2, No	LP, BP, HP, BR {NA}	------	------	------	NA	NA	NA	No
20.	2, DDCC 1, Amplifier	2/2, Yes	BP {L/H}	------	------	------	Yes	Yes	NA	Yes
21.	2, CDTA 1, CA	0/2, No	------	------	BP {L/H}	------	Yes	Yes	NA	Yes
22.	3, CDTA	1/2, Yes	------	------	LP, BP(C), HP(C) {L/L}	------	Yes	Yes	5.9	No
23.	4, ECCII	2/2, No	------	------	BP {L/L}	------	Yes	No	NA	No
24.	4, OFCC	5/2, Yes	------	------	BP {L/H}	------	Yes	No	NA	Yes
25.	2, CDTA	2/2, No	------	------	BP(C) {H/L}	------	Yes	No	7.79	No
26.	2, CDTA 1, TA	1/2, Yes	------	------	LP(R), BP {L/L}	------	Yes	Yes	21.2	No
27.	3, CC-CDCTA 1, CCII	0/2, No	------	------	UF {L/H}	------	Yes	Yes	2.23	Yes
28.	1, CCCTA, 1, EX-CCCTA	0/2, Yes	------	------	UF {L/H}	------	Yes	Yes	4.1	Yes
*29.	4, OFCC	5/2, No	------	BP{H/H}	------	BP {L/L}	No	No	NA	Yes
This work	2, FDCCCTA (Fig. 6)	0/3, 4 MOSs, Yes	LP, BP, HP, AP {L/H}	------	UF {H/H}	------	Yes	Yes	3.7	No
	2, FDCCCTA (Fig. 7)	1/3, 4 MOSs, Yes	LP, BP, HP, AP {H/H}	UF{H/H}	UF {H/H}	LP, BP, HP, AP {H/H}				No

NOTE: *Different structures are required to obtain each filter response; BP(C), HP(C) & LP (R): Represent the availability of responses through capacitors (C) and resistors (R); hence require additional circuitry for practical implementation; H: High; L: Low.

ity factor are 46.22 MHz and 1, respectively, while the simulated pre-layout and post-layout frequencies are 46.45 MHz and 45.98 MHz, respectively.

The simulation for the mixed-mode shadow filter of Fig. 7 is performed with the same parameters as used for the non-shadow filter along with $I_{B1}^{(2)} = I_{A1}^{(2)} = 40$ μA, $R_1 = R_2 = 1.38$ kΩ. The simulated gain responses of LP, HP, BP, and BR are shown in Fig. 13 (a), and the gain and the phase responses of AP are shown in Fig. 13 (b) for the VM and TIM. Similarly, the responses for CM and TAM are shown in Fig. 14. The simulated f_0 and the Q are 46.41 MHz and 1.1 vis-a-vis the calculated values of 46.41 MHz and 0.95.

The tunability of f_0 along with BW for constant Q can be obtained by varying $C_1 = C_3 = C$. The simulated responses for the mixed-mode shadow filter of Fig. 6, using C = 1 pF, 2 PF, and 4 pF, are shown in Fig. 15 (a). The simulated f_0s are obtained as 46.45 MHz, 23.19 MHz, and 11.75 MHz vis-à-vis the calculated values of 46.22 MHz, 23.11 MHz, and 11.55 MHz, respectively. The simulated BWs are 46.41 MHz, 23.42 MHz, and 11.86 MHz vis-à-vis the calculated BWs are 46.68 MHz, 23.34 MHz, and 11.66 MHz, respectively. Fig. 15 (b) shows the tunability

of the quality factor along with the gain of the BP filter by the variation of gain A_1, i.e., varying $g_{mB}^{(2)}$ in line with (46). The resulted quality factors are 0.8, 1.1, 1.3 and the gains are -1.2 dB, +1.4 dB, +3.7 dB for $I_{B1}^{(2)} = 40\ \mu A, 200\ \mu A$, and $400\ \mu A$, respectively.

The performance of the circuit is affected due to the fabrication process and mismatch deviation which has been analysed for the BP output response. Monte Carlo (MC) simulation for 200 runs is performed by considering the deviation of standard parameters of MOSs. Fig. 16 (a) shows the MC results for the frequency response of BP in VM and TIM while Fig. 16 (b) shows for the same in CM and TAM. Fig. 17 (a) shows the histogram plot of the distribution of samples for center frequency in VM and TIM which results the standard deviation as 2.7 MHz. While, Fig. 17 (b) shows for the CM and TAM which results the standard deviation of 2.9 MHz.

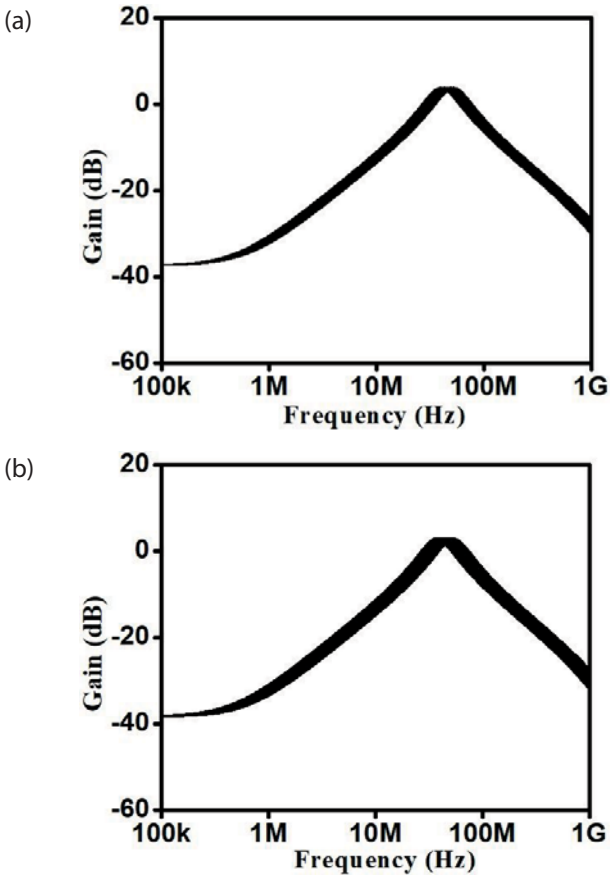

Figure 16: Monte Carlo simulation for 200 runs for BP output response (a) VM and TIM (b) CM and TAM.

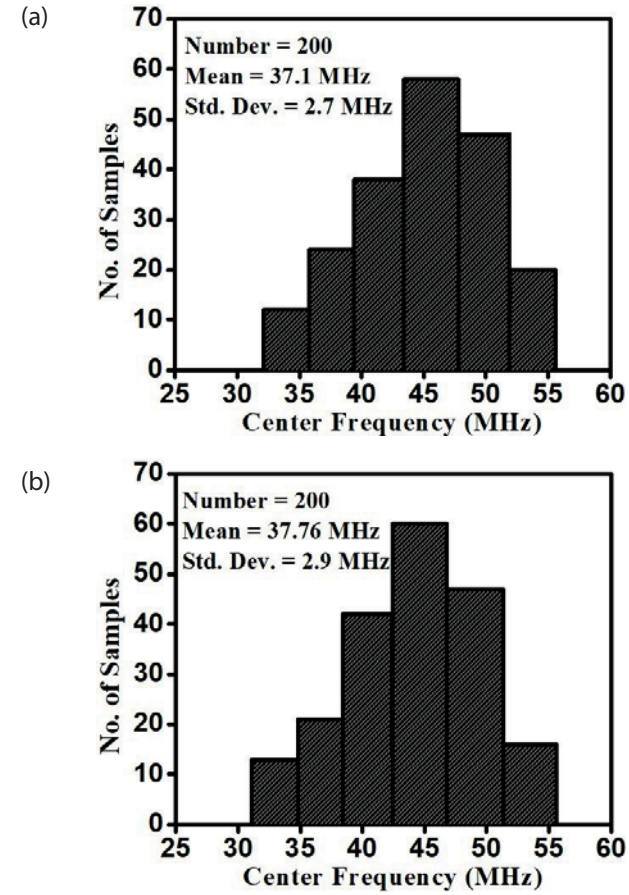

Figure 17: Statistical results of Monte Carlo simulation for BP output response (a) VM and TIM (b) CM and TAM.

The PVT analysis has also been done for the Fast Fast (FF), nominal, and Slow Slow (SS) corners. Voltage has been varied in the range of 1.2 V ± 10 %. Whereas, temperatures have been taken as -40 °C, 27 °C, and 125 °C for the FF, nominal, and SS corners, respectively. Fig. 18 (a) shows for all the three corners which results in the centre frequencies of 53.5 MHz, 46.41 MHz, 40.32 MHz in the FF, nominal, and SS corners, respectively in the VM and TIM mode. While, Fig. 18 (b) shows the similar results in CM and TAM mode which gives the centre frequencies as 55.7 MHz, 46.41 MHz, 39.97 MHz.

The measure of %THD (% total harmonic distortion) for the HP and LP mixed-mode shadow filter as a function of the input signal is shown in Fig. 19. The %THD variation is less than 5% for VM and CM filters up to 600mA and 1000mA, as shown in Fig. 19 (a) and Fig. 19 (b), respectively.

7 Conclusions

This paper presents a novel mixed-mode universal filter using a single active building block, FD-CCCTA, a new

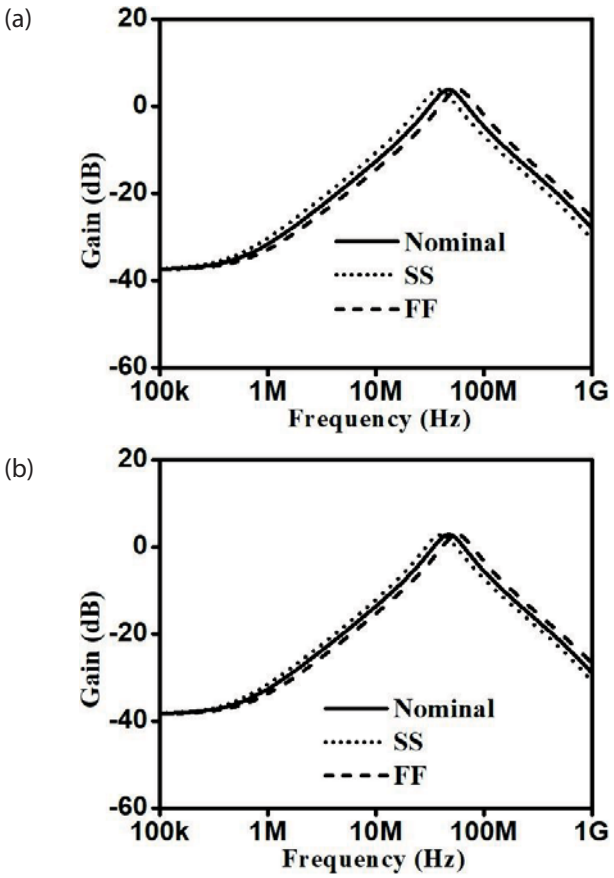

Figure 18: Simulated frequency responses of BP filter in fast, nominal, and slow corners (a) VM and TIM (b) CM and TAM.

variant of FD-CCII, and three capacitors. All the standard responses such as LP, BP, HP, BR, and AP are obtained in all VM, CM, TIM, and TAM modes. It is then extended to shadow filters to add flexibility in the orthogonal tuning of filter parameters, such as pole frequency (ω), quality factor (Q), and the tuning of the filter's gain. The first proposed shadow-filter circuit realizes the VM and CM UFs, while the second shadow filter realizes UFs for all the four modes, such as CM, TAM, VM, and TIM. To the best of the authors' knowledge, there is no reporting of a mixed-mode shadow filter in literature. The theoretical results are verified using TSMC 180 nm technology in Cadence Virtuoso Spectre.

8 Conflict of interest

The authors declare that there is no conflict of interest for this paper. Also, there are no funding supports for this manuscript.

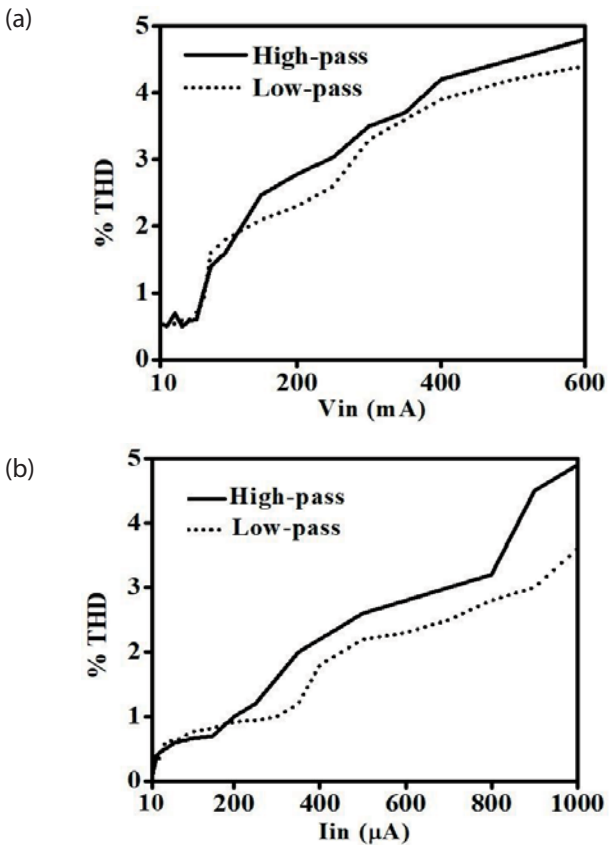

Figure 19: %THD variation of HP and LP Shadow filter (Fig. 6) (a) VM (b) CM.

9 References

1. M. Parvizi, "Design of a new low power MISO multi-mode universal biquad OTA-C filter," Int. J. Elec, vol. 106, no. 3, pp. 440-454, 2018,.
2. M. Kumngern, P. Suwanjan, K. Dejhan, "Electronically tunable voltage-mode universal filter with single-input five output using simple OTAs," Int. J. Elec, vol. 100, no. 8, pp. 1118-1133, 2012.
3. B. Chaturvedi, J. Mohan, A. Kumar, "A new versatile universal biquad configuration for emerging, signal processing applications," J.Circ. Syst. Comp, vol. 27, no. 12, pp. 1-28, 2018..
4. H. P. Chen, W. S. Yang, "Electronically tunable current controlled current conveyor transconductance amplifier-based mixed-mode biquadratic filter resistorless and grounded capacitors," Appl. Sci, vol. 7, pp. 1-22, 2017.
5. M.A. Ibrahim, "Design and analysis of a mixed-mode universal filter using dual-output operational transconductance amplifiers (DO-OTAs). Proceedings of the international conference on computer and communication engineering, pp. 915-918, 2008.
6. M. Kumngern, S. Junnapiya, "Mixed-mode universal filter using OTAs," Proceedings of the 2012 IEEE

international conference on cyber technology in automation, control and intelligent systems, pp. 119-122, 2012.
7. W.B. Liao, J.C. Gu, "SIMO type universal mixed-mode biquadratic filter." Indian Journal of Engineering & Materials Sciences, vol. 18, pp. 443-448.
8. S. Minaei, M.A. Ibrahim, "A mixed-mode KHN-biquad using DVCC and grounded passive elements suitable for direct cascading," Int. J. Circ. Theor. Appl, vol. 37, no. 7, pp. 793-810, 2009.
9. M. Parvizi, A. Taghizadeh, H. Mahmoodian, Z.D. Kozehkanani, "A low-power mixed-mode SIMO universal g_m-C filter," J. Circ. Syst. Comp, vol. 26, no. 10, pp. 1-16, 2017.
10. N.A. Shah, M.A. Malik, "Multifunction mixed-mode filter using FTFNs," Analog Integr. Circ. Sig. Process, vol. 47, pp. 339-343, 2006.
11. C.N. Lee, C.M. Chang, "Single FDCCII-based mixed-mode biquad filter with outputs," AEU-Int. J. Electron. Comm., vol. 63, pp. 736-742, 2009.
12. L. Zhijun, "Mixed-mode universal filter using MC-CCII," AEU-Int. J. Electron. Comm, vol. 63, pp. 1072-1075, 2009.
13. M.T. Abuelma'atti, N. Almutairi, "New CFOA-based shadow bandpass filter," In: 15th international conference on electronics, information, and communications, 2016.
14. M.T. Abuelma'atti, N. Almutairi, "New voltage-mode bandpass shadow filter," In: 13th international multi-conference on systems, signals & devices, pp. 412-415, 2016.
15. M.T. Abuelma'atti, N.R. Almutairi, "New current-feedback operational amplifier based shadow filters," Analog Integr. Circ. Sig. Process, vol. 86, pp. 471-480, 2016.
16. R. Anurag, R. Pandey, N. Pandey, M. Singh, M. Jain, "OTRA based shadow filters," Annual IEEE India Conference, 2016.
17. P. Huaihongthong, A. Chaichana, P. Suwanjan, S. Siripongdee, W. Sunthonkanokpong, P. Supavarasuwat, W. Jaikla, F. Khateb, "Single-input multiple-output voltage-mode shadow filter based on VDDDAs," AEU-Int. J. Electron. Commun, vol. 103, pp. 13-23.
18. F. Khateb, W. Jaikla, T. Kulej, M. Kumngern, D. Kubanek, "Shadow filters based on DDCC," IET Circuits Devices Syst, vol. 11, pp. 631-637, 2017.
19. S.C. Roy, "Shadow filters: a new family of electronically tunable filters," IETE J. Edu, vol. 51, pp. 75-78, 2010.
20. A. Yesil, F. Kacar, "Band-pass filter with high quality factor based on current differencing transconductance amplifier and current amplifier" AEU-Int. J. Electron. Commun, vol. 75, pp. 63-69, 2017.
21. A. Yesil, F. Kacar, S. Minaei, "Electronically controllable bandpass filters with high quality factor and reduced capacitor value: an additional approach" AEU-Int. J. Electron. Commun. vol. 70, pp. 936-943, 2016.
22. M. Atasoyu, H. Kuntman, B. Metin, N. Herencsar, O. Cicekoglu, "Design of current-mode class 1 frequency-agile filter employing CDTAs," European conference on circuit theory and design, 2015.
23. M. Atasoyu, B. Metin, H. Kuntman, N. Herencsar, "New current-mode class 1 frequency-agile filter for multi-protocol GPS application," Elektronika IR Elektrotechnika, vol. 21, pp. 35-39, 2015.
24. D. Nand, N. Pandey, "New configuration for OFCC-based CM SIMO filter and its application as shadow filter," Arab. J. Sci. Eng. Vol. 43, pp. 3011-3022, 2018.
25. N. Pandey, R. Pandey, R. Choudhary, A. Sayal, M. Tripathi, "Realization of CDTA based frequency agile filters," IEEE international conference on signal processing computing and control, 2013.
26. N. Pandey, A. Sayal, R. Choudhary, R. Pandey, "Design of CDTA and VDTA based frequency agile filters," Adv. Electron, pp. 1-14, 2014.
27. D. Singh, S.K. Paul, "Realization of current-mode universal shadow filter," AEU-Int. J. Electron. Commun, vol. 117, pp. 153088, 2020.
28. D. Singh, S.K. Paul, "Improved current-mode biquadratic shadow universal filter," Inf. MIDEM-J. Microelectron. Electron. Compon. Mater, vol. 52, no. 1, pp. 51-66, 2022.
29. D. Nand, N. Pandey, V. Bhanoo, A. Gangal, "Operational floating current conveyor based TAM & TIM shadow filter," Proceedings of 4th international conference on computer and management ICCM, pp. 103-115, 2018.
30. F. Gur, F. Anday, "Simulation of a novel current-mode universal filter using FDCCIIs," Analog Integr. Circ. Sig. Process, vol. 60, pp. 231-236, 2009.
31. Y. Lakys, A. Fabre, "Shadow filters-new family of second order filters," Electron Lett, vol. 46, no. 4, pp. 985-986, 2010.
32. V. Biolkova, D. Biolek, "Shadow filters for orthogonal modification of characteristics frequency and bandwidth," Electronics Letters, vol. 46, no. 12, pp. 830-831, 2010.
33. M. Kumngern, T. Nonthaputha, F. Khateb, "Arbitrary waveform generators using current-controlled current conveyor transconductance amplifier and current conveyor analog switches," J. Circ. Syst. Comp, vol. 28, no. 11, pp. 1950179, 2019.

Arrived: 31. 07. 2022
Accepted: 24. 11. 2022